Cao *et al. BMC Biology* (2024) 22:293
https://doi.org/10.1186/s12915-024-02088-5

BMC Biology

RESEARCH ARTICLE

Open Access

Type-B response regulator RRB12 regulates nodule formation in *Lotus japonicus*

Jingjing Cao[1†], Yu Zhou[1,2†], Tao Tian[1†], Jie Ji[1†], Yan Deng[1], Yuhao Guan[1], Yongmei Qi[1], Longxiang Wang[1,3], Longlong Wang[1,4], Yibo Huang[1], Qiuling Fan[5] and Deqiang Duanmu[1,5,6*]

Abstract

Background The mutualistic beneficial relationship between legume plants and rhizobia enables the growth of plants in nitrogen-limiting conditions. Rhizobia infect legumes through root hairs and trigger nodule organogenesis in the cortex. The plant hormone cytokinin plays a pivotal role in regulating both rhizobial infection and the initiation of nodule development. However, the mechanism used by the cytokinin output module to control symbiosis remains poorly documented.

Results In this study, we identified a cytokinin signaling output component encoded by the *Type-B RESPONSE REGULATOR* (*RRB*) gene, *LjRRB12*, which is expressed in *Lotus japonicus* nodule primordia and young nodules. Disruption of *LjRRB12* leads to a reduction in nodulation and to an increase in the number of infection threads. Overexpression of LjRRB12^{D76E}, an active form of the LjRRB12 protein, induces nodule-like structures in wild type and *hit1* (*hyperinfected 1/lotus histidine kinase 1*) mutants but not in *nin2* (*nodule inception 2*) mutants. Additionally, we utilized nCUT&Tag and EMSA to demonstrate that LjRRB12 can bind a CE (cytokinin response element) from the *LjNIN* promoter.

Conclusions Our results provide a deeper understanding of nodule organogenesis by establishing a link between the cytokinin signal and the transcriptional regulation of *LjNIN*.

Keywords Cytokinin, Type-B response regulator, Nodule inception, Symbiotic nitrogen fixation, Infection thread, Nodule organogenesis

[†]Jingjing Cao, Yu Zhou, Tao Tian and Jie Ji contributed equally to this work.

*Correspondence:
Deqiang Duanmu
duanmu@mail.hzau.edu.cn
[1] State Key Laboratory of Agricultural Microbiology, Hubei Hongshan Laboratory, Huazhong Agricultural University, Wuhan 430070, China
[2] School of Biological and Food Engineering, Engineering Research Center for Development and High Value Utilization of Genuine Medicinal Materials in North Anhui Province, Suzhou University, Suzhou, Anhui 234000, China
[3] College of Life Sciences, Zhejiang Normal University, Jinhua, Zhejiang 321004, China
[4] College of Agronomy, Anhui Agricultural University, Hefei 230036, China
[5] College of Life Science and Technology, Huazhong Agricultural University, Wuhan 430070, China
[6] Shenzhen Branch, Guangdong Laboratory for Lingnan Modern Agriculture, Genome Analysis Laboratory of the Ministry of Agriculture, Agricultural Genomics Institute at Shenzhen, Chinese Academy of Agricultural Sciences, Shenzhen 518000, China

Background

Legumes have evolved particular nitrogen-fixing organs called root nodules which provide an ideal microoxic environment for the nitrogen-fixing activity of intracellular symbiotic rhizobia. The crosstalk between rhizobia and legume plants begins with flavonoids secreted by plant roots [1, 2] and nodulation factors (NFs), lipochitooligosaccharide molecules produced by rhizobia [3, 4]. The Nod Factor Receptor 1/5 (NFR1/NFR5) complex on the plant membrane perceives NF and triggers plant responses, including cytoplasm and nuclear Ca^{2+} spiking [5, 6], cytoskeleton rearrangements [7], and plant cell wall degradation [8], all of which are crucial for the initiation and progression of infection threads in legume plants [9]. Nuclear calcium oscillations trigger a transcriptional regulatory cascade associated with the symbiotic process [9, 10]. Several transcription factors, such as LjCYCLOPS/Interacting Protein of DMI3 (MtIPD3) [11, 12], ERF Required for Nodulation (ERN) [13, 14], Nodulation Signaling Pathway 1 (NSP1) and NSP2 [15–17], and Nodule Inception (NIN) [18–20] are indispensable for the NF-induced transcriptional network and IT progression.

Root nodule formation arises from cortical or endodermal cells in the root differentiation zone and requires these cells to re-enter mitotic division and undergo dedifferentiation [21–23]. Cortical cell division occurs before IT penetrates the epidermal layer, suggesting that a mobile signal connects the infection and nodulation organogenesis programs [9]. However, at the early stage, the Ca^{2+} spiking signal induced by NF is immobile and confined to the epidermis [19]. Cytokinin, a plant hormone, may serve as one of the potential mobile signals that relay symbiotic signals from the epidermis to the cortex. Cytokinin plays a significant role in various symbiotic processes [24, 25]. Endogenous bioactive cytokinin levels were enhanced during the early nodulation stage [26, 27]. Several cytokinin synthesis and signaling-related genes, including Isopentenyl Transferase (*LjIPT*) and Lonely Guys (*LjLOG*) [27], cytokinin transporter ATP-binding cassette (ABC) gene *MtABCG56* [28], cytokinin receptor Histidine Kinase 1 (*LjLHK1*) [29, 30], and the synthetic cytokinin response reporter Two-Component Signaling Sensor (*LjTCS*) or *LjTCSnew* [27, 29], are transcriptionally upregulated in response to the rhizobial infection.

Cytokinin regulates several rhizobia-induced nodule specific genes such as *MtNSP2*, *MtNIN*/*LjNIN* and *MtNF-YA1*/*LjNF-YA1* [31–35]. The essential role of cytokinin signaling in infection and nodulation was supported by the symbiotic phenotypes of two *L. japonicus ljlhk1* mutants, the loss-of-function hyperinfected 1 (*hit1*) [30] and the gain-of-function spontaneous nodule formation 2 (*snf2*) mutants [36]. In *hit1* roots, nodulation is aborted even though the root hairs are hyperinfected [30]. Conversely, spontaneous nodulation occurred in *snf2* roots in the absence of rhizobia [36]. These distinct phenotypic differences underscore that the cytokinin signal is both essential and sufficient for dedifferentiation and cell division, ultimately leading to nodulation. Cytokinin accumulation is tightly regulated and cytokinin homeostasis is required for efficient infection, nodule organogenesis, and regulation of nitrogen fixation in mature nodules [26, 37, 38]. Cytokinin also participates in the nitrogen fixation-senescence transition in *Medicago truncatula* nodules [39].

Sinorhizobium meliloti-induced symbiotic signaling genes in *M. truncatula* are dependent on *MtCRE1* and *MtNIN* [34]. Overexpression of *MtNIN* in the cortex of *cre1* is sufficient to induce cell division and nodule formation, indicating that *MtNIN* functions downstream of *MtCRE1* [19]. Further studies showed that *LjLHK1*/*MtCRE1*-dependent cytokinin signaling was required for the cortical expression of *NIN*, which is indispensable for the initiation and development of nodule primordia [19, 33]. A conserved *cis*-regulatory element in the distal region of the *NIN* promoter, known as the cytokinin response element-containing region (CE), was found to be necessary for *MtNIN* expression in the cortex and pericycle layers, and it contains the putative core binding site for type-B response regulators (RRBs) [33]. While the genetic association of cytokinin signaling and symbiotic signaling has been well established, the mechanism by which cytokinin signaling output modules, particularly the RRBs, affect symbiotic nitrogen fixation remains unclear.

In higher plants, the transduction of cytokinin signaling depends on a His-Asp phosphorelay system, which is commonly observed in bacterial two-component signaling pathways [40]. The extracellular CHASE (cyclases/histidine kinases associated sensory extracellular) domain of Histidine Kinase recognizes cytokinin and triggers the transfer of a phosphate group to His-containing Phosphotransferase (HP) and Response Regulator (RR) [41–43]. Based on these conserved domain structures, RRs are classified into four groups including A, B, C-type RRs, and pseudo-RRs [44, 45]. *Arabidopsis thaliana* RRBs, the key transcription factors involved in cytokinin signal transduction, contain a receiver domain in the N-terminal region, a Myb-like domain for DNA binding, and a proline-rich region in the C-terminal region [46]. RRBs serve as connectors between cytokinin signaling and other pathways and play major roles in regulating cell proliferation throughout plant development [45, 47, 48].

In *M. truncatula*, RRBs directly activate the expression of *MtNSP2*, basic Helix-Loop-Helix (*MtbHLH*) and Anaphase-Promoting Complex (APC) activator Cell Cycle Switch 52A (*MtCCS52A*), thereby initiating a transcriptional network to promote nodule formation [35, 49]. However, the specific roles of RRBs in symbiosis are not fully understood. In this study, we identified an *RRB* gene, *LjRRB12* in the Arabidopsis ARR10/ARR12 subclade that is not orthologous to the previously characterized *MtRRB1* and *MtRRB3* genes. *LjRRB12* is expressed at the onset of root cortical cell division. Phenotypic characterization of two *LORE1* insertional mutants of *LjRRB12* and roots that overexpressed *LjRRB12* revealed that *LjRRB12* may play a positive role in nodulation and a negative role in epidermal infection. Our data additionally show that LjRRB12 may regulate the expression of *LjNIN* by interacting with a remote element in the *LjNIN* promoter. This study unveils a new member in the cytokinin signaling pathway that contributes to rhizobial infection and nodule organogenesis.

Results

Identification of *LjRRB* genes from *Lotus japonicus*

To identify *RRB* genes in *L. japonicus*, the amino acid sequences of *A. thaliana* ARR1 and ARR2 were used as BLAST queries of the *L. japonicus* Gifu v1.3 genome [50] available in Lotus Base [51]. We identified ten *L. japonicus RRB* genes, each containing a phosphoreceiver domain and a Myb-like DNA-binding domain (Additional file 1: Fig. S1 and Additional file 2: Table S1). A phylogenetic tree was constructed to compare the LjRRBs with known RRBs from *M. truncatula* and *A. thaliana* (Fig. 1). RRB proteins comprise six subfamilies, as previously reported [52]. In *A. thaliana*, the ARR10/ARR12/ARR18 and ARR1/ARR2 clades are the most well-characterized RRB subfamilies [53–55]. Two members of the ARR10/ARR12/ARR18 clade in *M. truncatula* named MtRRB1 and MtRRB3 have been well studied (Fig. 1) [35, 49]. Consistent with previous observations in *M. truncatula* [56], an expansion of the gene number within the ARR10/ARR12/ARR18 clade was also observed in *L. japonicus* (Fig. 1), which is consistent with a role for this clade in symbiosis. In *L. japonicus*, the ARR10/ARR12/ARR18 clade includes six LjRRBs, with four LjRRBs more closely related to MtRRB1/MtRRB3, one LjRRB (LotjaGi1g1v0572600_LC.1) in the early branching within this clade, and the last one (LotjaGi6g1v0205900.1) closely related to ARR12/ARR10 (Fig. 1). LotjaGi6g1v0205900.1 shared the most sequence similarity with Arabidopsis ARR12, and was therefore named LjRRB12. The amino acids essential for the phosphorelay in Arabidopsis ARR1 (D44, D89, K138) are conserved in LjRRB12. In contrast, we observed an Aspartate to Asparagine substitution in LotjaGi1g1v0572600_LC.1 (Additional file 1: Fig. S1). The focus of this research was then directed towards characterizing the influence of LjRRB12 on symbiosis.

Expression pattern of *LjRRB12* during nodule organogenesis

To confirm whether the expression of *LjRRB12* correlates with nodule development, a spatiotemporal expression analysis was conducted through histochemical staining. A reporter gene (*pLjRRB12::GUS*) containing the 3-kb *LjRRB12* promoter driving the expression of a β-glucuronidase (GUS) reporter gene was introduced into *L. japonicus* by hairy root transformation. Basal activity of the *LjRRB12* promoter was detectable in the root apex (Fig. 2A) and vascular tissues of uninoculated roots (Fig. 2B,C). In uninoculated roots, GUS activity was undetectable in the root cortex in the susceptible zone (Fig. 2B,C). At the early stage of infection, GUS activity was detected in the dividing root cortical cell layers at 3 dpi (Fig. 2D) and in the developing nodule primordium at 5 dpi (Fig. 2E, I) and 7 dpi (Fig. 2F, J).

At the later stages of nodule development, *LjRRB12* promoter-driven GUS expression was confined to the cortical layer of young nodules (14 dpi) (Fig. 2G, K) and was ultimately limited to the vascular bundles of fully mature nodules (21 dpi) (Fig. 2H, L). Cross-sections confirmed the absence of detectable GUS activity in the nitrogen-fixing region of both pre-mature and mature nodules (Fig. 2K,L). Taken together, our results provide evidence that rhizobial inoculation induces the expression of *LjRRB12* in the root cortical cells and subsequently in the cortex tissues of the outer nodule.

LjRRB12 positively regulates nodule organogenesis and negatively regulates rhizobial infection

Several studies reported that cytokinin acts as a bifunctional regulator, negatively affecting rhizobial infection in the epidermal layer and positively regulating nodule development in the cortex cell layer [30, 33]. To determine the role of *LjRRB12* in symbiosis, we obtained *ljrrb12* mutants from a *LORE1* insertion mutant library [57]. Two mutant lines, namely *ljrrb12-1* and *ljrrb12-2*, were identified, harboring a *LORE1* insertion either in the 5′ UTR (*ljrrb12-1*) or in exon1 (*ljrrb12-2*) (Fig. 3A,B). The mRNA levels of *LjRRB12* in the roots from *ljrrb12-1* and *ljrrb12-2* mutants were significantly reduced, reaching only 12% and 22% of the levels in Gifu plants, respectively (Fig. 3C). At 5 dpi, ITs successfully crossed over the epidermal cells and reached the cortex cells in Gifu roots (Fig. 3D,E). In contrast, a significant number of ITs in both mutants followed aberrant paths within the root epidermis (Fig. 3F–I). As a result, the frequency of

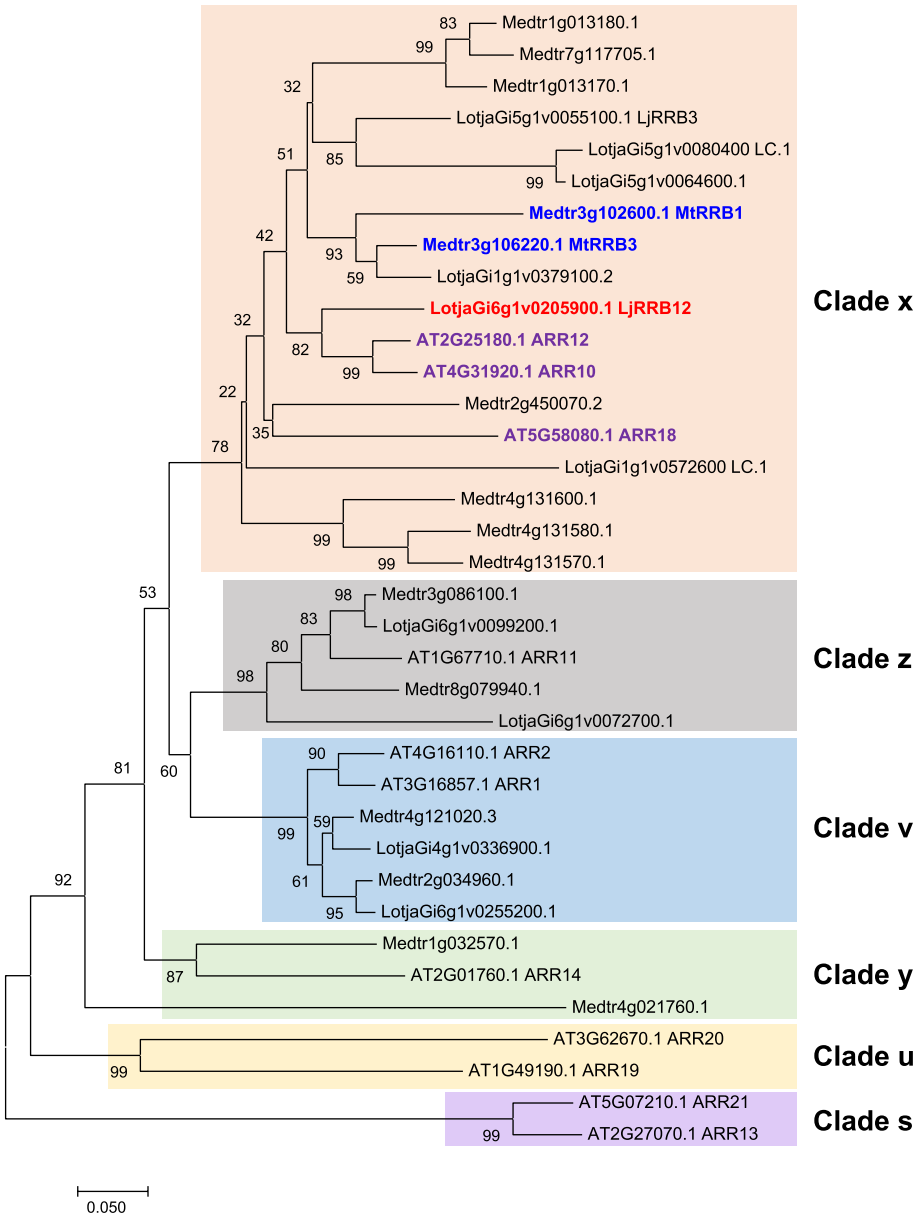

Fig. 1 Phylogenetic analysis of type-B response regulators. Phylogenetic tree analysis of RRBs from *Arabidopsis thaliana*, *Lotus japonicus*, and *Medicago truncatula*. The conserved receiver domains of RRBs were used to construct an evolutionary tree using a Neighbor-Joining method and 1000 bootstrap replicates with MEGA 11. The scale bar indicates the number of amino acid substitutions per site

microcolony and epidermal infection threads (eITs) was notably increased by ~45% in the *ljrrb12* mutants relative to WT (Fig. 3K). While most ITs failed to induce cortical cell division, a small number of ITs escaped the epidermal arrest and successfully induced the initiation of nodule meristems (Fig. 3F). Overall, formation of nodule primordia (NP) occurred at a lower frequency in the mutant plants, with rates of 77% for *ljrrb12-1* and 75% for *ljrrb12-2* compared to WT (Fig. 3L).

The phenotype of decreased nodulation and increased epidermal infection in the *ljrrb12* mutants is consistent with the effects of cytokinin on epidermal infection and early-stage nodulation that were reported previously [30]. At a later symbiotic stage, the shoot fresh weight (FW) of *ljrrb12-1* and *ljrrb12-2* mutants was significantly reduced compared to WT (Fig. 4A,B). The nodule number and ARA activity of the two *ljrrb12* mutants, either normalized on a per plant or per nodule fresh weight basis, were also significantly reduced (Fig. 4C–E). Taken together,

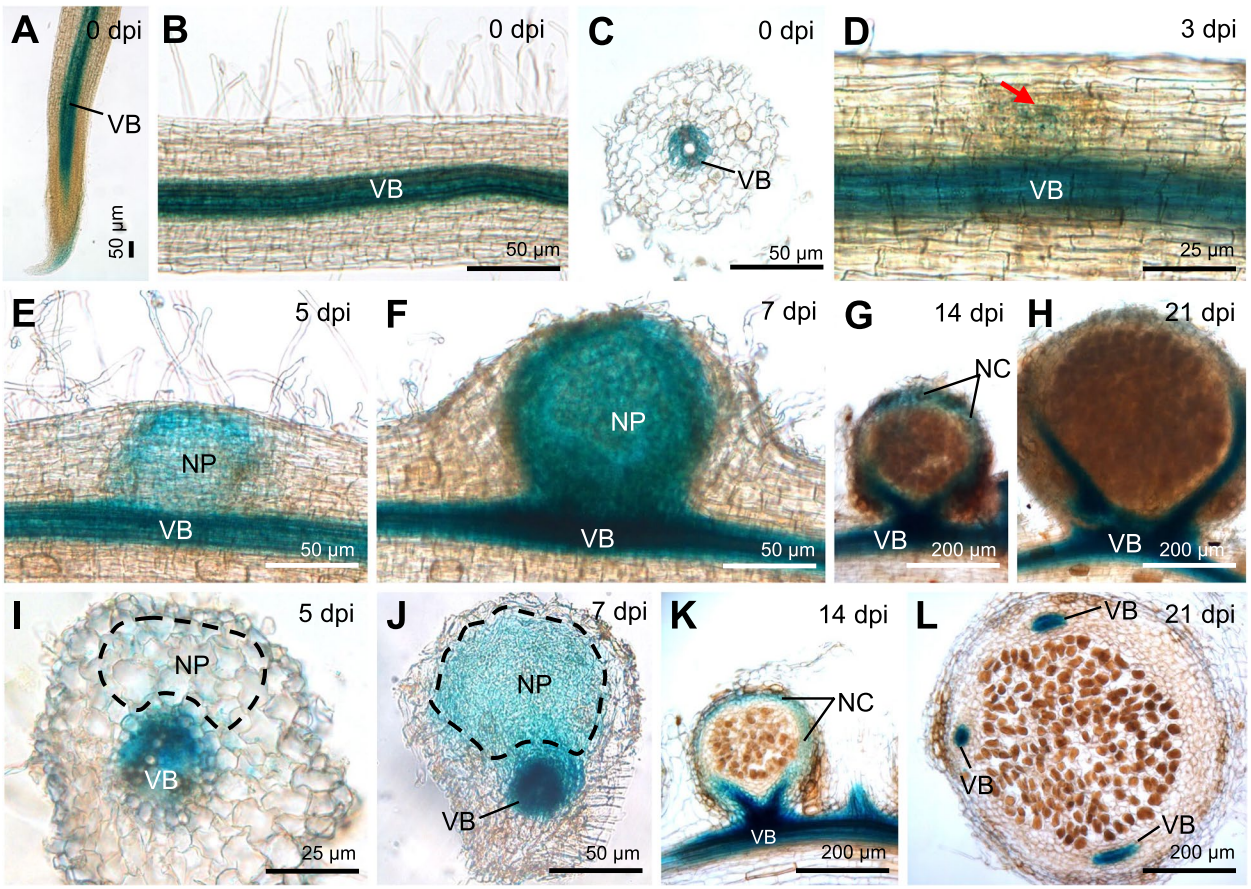

Fig. 2 Analysis of *LjRRB12*promoter activity at different stages of nodule development. Promoter activity was assayed by staining for GUS activity using hairy roots harboring the *pLjRRB12::GUS* reporter geneat different stages of nodule development, including roots at 0 dpi (**A**–**C**), nodule primordia at 3 and 5 dpi (**D**, **E**, **I**), young nodules at 7 and 14 dpi (**F**, **G**, **J**, **K**), and mature nodules at 21 dpi (**H**, **L**). The red arrow indicates a nodule primordium in **D**. Images are representative of at least ten independent transgenic plants. VB, vascular bundle; NC, nodule cortex; NP, nodule primordium. Scale bars, 25 μm (**D**, **I**), 50 μm (**A**–**C**, **E**, **F**, **J**), and 200 μm (**G**, **H**, **K**, **L**)

these results are consistent with *LjRRB12* affecting nodule numbers and the nitrogen fixation activity of mature nodules.

The symbiotic gene *LjNIN* is transcriptionally regulated by LjRRB12

We next investigated how expression of the key cytokinin signaling and the symbiotic signaling pathway genes was affected in the *ljrrb12-1* mutant. Roots of mutant and wild-type Gifu plants were treated with 10^{-7} M 6-Benzylaminopurine (6-BA) for 1 h and harvested for an RT-qPCR analysis. The expression of *LjRRB12* was not induced by cytokinin (Fig. 5A), which is consistent with the observation in *A. thaliana* that the mRNA levels of many B-type response regulators, including ARR1/ARR2/ARR10, are not induced by cytokinin [58]. The mRNA level of the cytokinin receptor gene *LjLHK1* was upregulated by cytokinin in Gifu roots. This upregulation also occurred in *ljrrb12-1* and the mRNA levels after cytokinin treatment did not differ significantly between *ljrrb12-1* and Gifu (Fig. 5A). Without a cytokinin treatment, the transcript abundance of the cytokinin response gene *LjRRA5* (a type A RR, also named as *LRR5*) [30] was significantly higher in the *ljrrb12-1* mutant compared to Gifu, whereas after the cytokinin treatment, the expression of *LjRRA5* was similar in the two genotypes (Fig. 5A).

Among the symbiotic signaling genes, expression of *LjNSP2* was inhibited by a cytokinin treatment in Gifu (Fig. 5B), consistent with the previous results in *L. japonicus* [31]. The expression of *LjNSP2* was significantly higher in the *ljrrb12-1* mutant than in Gifu and was insensitive to the cytokinin treatment (Fig. 5B). Consistent with previous studies [31], *LjNIN* and *LjNF-YA1* were upregulated by the cytokinin treatment (Fig. 5B). The expression of *LjNIN* was significantly reduced in the *ljrrb12-1* mutant relative to Gifu after the cytokinin treatment (Fig. 5B). However, there was no significant

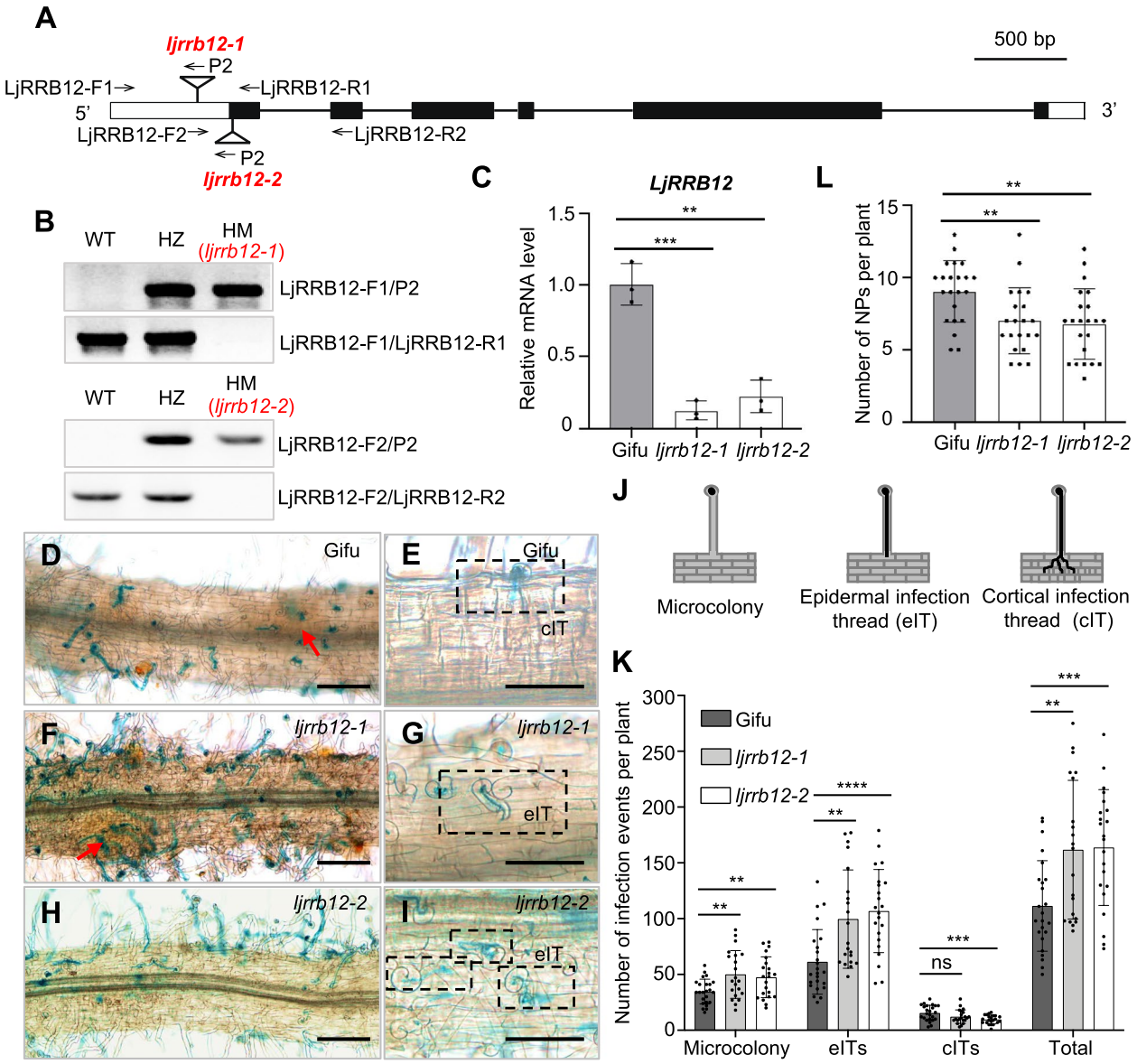

Fig. 3 Symbiotic nitrogen fixation phenotype of the *ljrrb12* mutants. **A** Gene structure of *LjRRB12* and *LORE1* insertion sites in the *ljrrb12-1* and *ljrrb12-2* mutants. Black boxes, white boxes, lines, triangles and arrows indicate exons, 5' and 3' untranslated regions (UTR), introns, *LORE1* insertions, and PCR genotyping primers, respectively. Scale bar represents 500 base pairs. **B** Identification of the *LORE1* insertion mutants using PCR and specific primers (Additional File 3: Table S2). WT, wild type; HZ, heterozygous mutant; HM, homozygous mutant. **C** Expression of *LjRRB12*in Gifu, *ljrrb12-1*, and *ljrrb12-2* mutants. Relative mRNA levels were normalized to *LjUBQ1*. The values are means ± SD from three biological replicates. **D**–**I** Infection and early nodulation phenotype of Gifu,*ljrrb12-1* and *ljrrb12-2* mutants. Roots were inoculated with *M. loti* NZP2235 (*hemA::lacZ*) and the symbiotic phenotype was analyzed. Representative images of roots from Gifu (**D**, **E**), *ljrrb12-1* (**F**, **G**), and *ljrrb12-2* (**H**, **I**) at 5 dpi are shown. Rhizobia were visualized using X-Gal staining. Red arrows indicate nodule primordia. A normal infection thread that crossed an epidermal cell and reached the underlying dividing cortical cells is shown (**E**). Arrested or mis-guided infection threads are shown (**G**, **I**). Scale bars, 100 μm. **J** Diagrams of different infection progresses. Left panel, bacterial microcolony inside a curling root hair; Middle panel, elongating infection thread in the epidermal layer (eIT, epidermal infection thread); Right panel, infection thread reaches the cortical cell layer (cIT, cortical infection thread). **K** Number of infection events in Gifu, *ljrrb12-1*,and*ljrrb12-2* mutants at 5 dpi, including microcolony, eITs, cITs, and the total number. **L** Number of nodule primordia (NP) per plant at 5 dpi. In **K** and **L**, values are means ± SD (n =21~24). A non-parametric test was used for statistical comparisons in **C**, **K**, **L**. ns, not significant; **,$P < 0.01$; ***, $P < 0.001$; ****, $P < 0.0001$

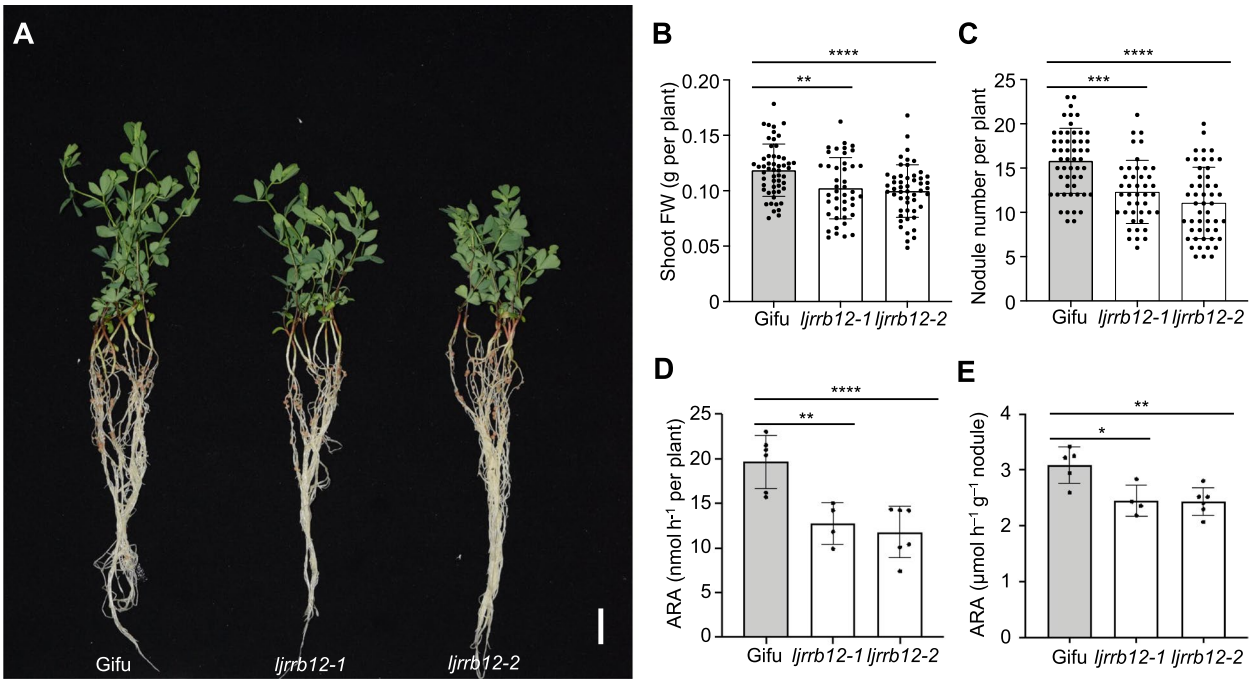

Fig. 4 *LjRRB12* deficiency inhibits nitrogen fixing activity in maturenodules. **A** Representative images of Gifu, *ljrrb12-1* and *ljrrb12-2* plants at 28 dpi. Scale bars, 1 cm. **B**,**C** Shoot fresh weight (FW) and nodule number of Gifu and the *ljrrb12* mutants at 28 dpi. Values in **B** and **C** are means± SD ($n = 43$~54). Student's *t* test was used for the statistical comparisons between Gifu and each mutant. **D**,**E** ARA (acetylene reduction assay) activity per plant (**D**) or per nodule fresh weight (**E**) of Gifu and the*ljrrb12* mutants at 28 dpi. Values in **D** and **E** are means ± SD ($n = 4$~6). A non-parametric test was used for the statistical comparisons between Gifu and each mutant. *, $P < 0.05$; **, $P < 0.01$; ***, $P < 0.001$; ****, $P < 0.0001$

difference in the expression of *LjNF-YA1* in cytokinin-treated WT and *ljrrb12-1* roots (Fig. 5B), indicating that cytokinin-triggered *LjNF-YA1* expression is independent of LjRRB12 and might be associated with other cytokinin downstream signaling. We also analyzed the expression of *CLAVATA3/ESR* (*CLE*)*-RELATED-ROOT SIGNAL* (*CLE-RS*) genes, which inhibit the formation of excess infection threads [59]. We found that all three genes were upregulated by the cytokinin treatment in Gifu. *LjCLE-RS1* and *LjCLE-RS2* were also upregulated in *ljrrb12-1*, but the mRNA levels were lower relative to Gifu after the cytokinin treatment, indicating a potential upregulation of *LjCLE-RS1* and *LjCLE-RS2* by LjRRB12 upon stimulation with cytokinin. Moreover, *LjCLE-RS3* was not cytokinin-inducible in *ljrrb12-1* (Additional file 1: Fig. S2).

LjRRB12 interacts with the *LjNIN* promoter

Based on the reduction in *LjNIN* expression after the cytokinin treatment in the *ljrrb12-1* mutant (Fig. 5B), we investigated whether *LjNIN* is a direct target of LjRRB12. The *LjNIN* promoter contains two previously reported conserved *cis* elements: one is the CYCLOPS Response Element (CYC-RE), which is essential for the epidermal expression of *NIN* in regulating IT formation [12, 33]; the other is the cytokinin response element (CE) required for the expression of *NIN* in the endodermis or pericycle layers and that was predicted to serve as an RRB binding site [33, 60]. Analysis of the *LjNIN* promoter revealed three conserved regions that are present in the promoters of various legume *NIN* genes but are absent from the promoters of *L. japonicus* NIN-like protein (*LjNLP*) genes (Additional file 1: Fig. S3) [33, 61].

The D1 and D3 region of the CE element contains several putative RRB binding motifs (Fig. 5C) [33, 60]. To clarify whether the LjRRB12 binding sites are enriched in the D1 or D3 regions of *LjNIN*, we employed a PCR-assisted SELEX (Systematic Evolution of Ligands by EXponential enrichment) assay to identify the binding motif of LjRRB12. After eight rounds of enrichment, individual clones were randomly selected for sequencing. The sequences were analyzed using MEME [62] and a 6-bp consensus sequence [5′-(A/T)GAT(A/T)(C/T)−3′, or the reverse complement 5′-(G/A)(A/T)ATC(A/T)−3′] was identified (Additional file 1: Fig. S4A-B). By comparing the core 6-bp LjRRB12 binding site and a more conserved core 5′-AGAT-3′, eight and three of such potential binding sites (LjRRB12BSs) were found in the D1 and D3 regions, respectively (Fig. 5C).

To verify whether LjRRB12 binds to the *LjNIN* promoter in vivo, we isolated nuclei from transgenic

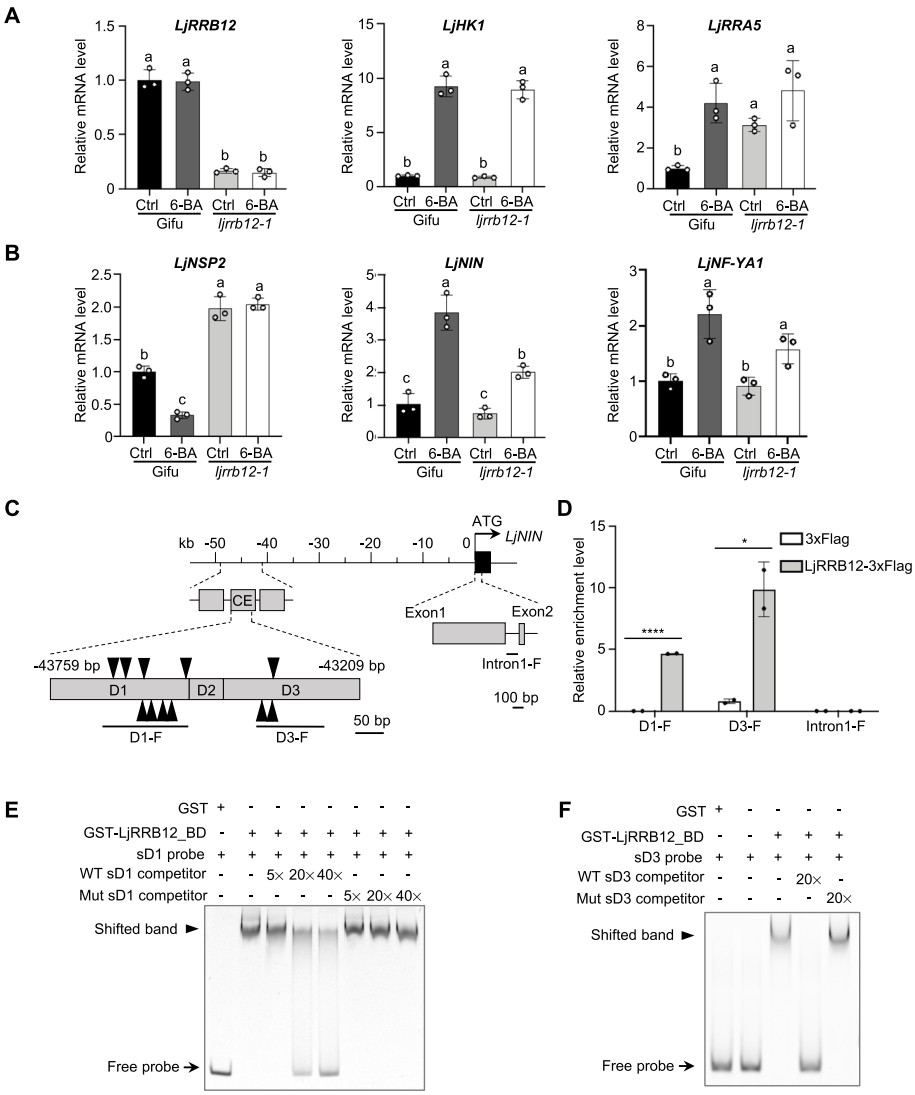

Fig. 5 Interactions between LjRRB12 and the D1 and D3 *cis*-elements of the *LjNIN* promoter. **A**,**B** Expression analysis of genes associated with cytokinin signaling (**A**) and symbiotic signaling (**B**) in Gifu and *ljrrb12-1* roots after the exogenous cytokinin treatment for 1 h. 6-Benzylaminopurine (6-BA) was added at a final concentration of 10^{-7} M. Relative expression levels were normalized to *LjUBQ1* expression levels. Data in **A** and **B** indicate means ± SD of three biological replicates. Statistical analysis was performed using Tukey's multiple comparison test. Means labeled with the same letter are not significantly different (i.e., $P < 0.05$). Ctrl, Control. **C** Diagram of the CE (cytokinin response element) region in the *LjNIN* promoter and the putative LjRRB12 binding motif in the CE. Black triangles indicate the binding motif 5′-(A/T)GAT(A/T)(C/T)-3′. DNA fragments in the D1 region (D1-F), D3 region (D3-F), and the first intron of *NIN* (Intron1-F) were used for nCUT&Tag-qPCR. Scale bars, 50 bp (in the CE region) or 100 bp (in the exon and intron region). **D** Enrichment levels of the LjRRB12 binding sites. An anti-Flag antibody was used to pull down DNA fragments from the transgenic hairy roots expressing LjRRB12-3×Flag (or 3×Flag as the control), and qPCR analyses were performed using appropriate primer pairs. The relative enrichment level of DNA was calculated by normalizing against the amount of standard DNA in the assay kit (5 pg in each sample). Data indicate mean values ± SD calculated using two biological replicates. A non-parametric test was used for statistical analysis. *, $P < 0.05$; ****, $P < 0.0001$. **E**,**F** EMSA (electrophoretic mobility shift assay) analysis for the binding of GST-LjRRB12_BD (BD, DNA binding domain) fusion protein to the *NIN* promoter, using either a short D1 (sD1, 146 bp) (**E**and Additional file 1: Fig. S4C) or short D3 (sD3, 111 bp) (**F**and Additional file 1: Fig. S4C) region. FAM-labeled sD1 and sD3 were used as probes. Unlabeled competitors (WT, wild type sequence; Mut, mutated sequence, Additional file 1: Fig. S4C) were used at 5-, 20-, and 40-fold (**E**) and at 20-fold (**F**) molar excess relative to the labeled probe. Arrows indicate the labeled free probes. Arrowheads indicate the shifted bands

hairy roots of Gifu overexpressing 3×Flag (EV) or LjRRB12-3×Flag for the nCUT&Tag assay. Fragments of the D1 and D3 regions were significantly enriched in the LjRRB12-3×Flag transgenic roots relative to the EV roots using sequences from the first intron as an endogenous negative control for qPCR (Fig. 5D). To further

confirm the interaction between LjRRB12 and the D1 and D3 regions, we performed an electrophoretic mobility shift assay (EMSA) experiment (Fig. 5E,F). The GST-tagged DNA binding domain of the LjRRB12 protein (GST-LjRRB12_BD) was expressed and purified from *Escherichia coli*. 5-Carboxyfluorescein (FAM)-labeled D1 and D3 fragments were produced and incubated with GST-LjRRB12_BD, resulting in bands with shifted mobilities (Fig. 5E,F). The addition of excess unlabeled competitor probes drastically reduced the abundance of the shifted bands, whereas the mutant competitors had no such effects (Fig. 5E,F). These data make the case that LjRRB12 binds the D1 or D3 regions of the *LjNIN* promoter both in vitro and in vivo.

To investigate whether a spatiotemporal colocalization exists between *LjRRB12* and *LjNIN*, the distant CE region and the ~ 5 kb proximal promoter (*CE-NIN*$_{5K}$) were fused to a GUS reporter gene and the expression cassette was introduced into *L. japonicus* Gifu using a hairy root transformation procedure. GUS staining was detectable in the dividing root cortical cell layers at 3 dpi (Additional file 1: Fig. S5A), the developing nodule primordium at 5 and 7 dpi (Additional file 1: Fig. S5B-C), and the cortex and infection zone of young and mature nodules at 14 and 21 dpi (Additional file 1: Fig. S5D-E). The spatiotemporal colocalization of *LjNIN* and *LjRRB12* in the root cortical cells and nodule primordium (Fig. 2D–F) provides evidence that they may interact in planta at the early symbiotic stage and that these interactions contribute to the regulation of infection and/or organogenesis.

Overexpression of LjRRB12 leads to the spontaneous formation of nodule-like structures in the absence of rhizobium

Exogenous cytokinin and the autoactivated cytokinin receptor LjLHK1^{L266F} were previously demonstrated to induce nodule-like structures in the absence of rhizobial inoculation [36, 63, 64]. To verify the role of LjRRB12 in the regulation of nodulation, we used hairy root transformation to transiently express LjRRB12 and its phosphomimic variant LjRRB12^{D76E} without rhizobial infection. Our findings revealed that expression of both LjRRB12 and LjRRB12^{D76E} in wild-type Gifu roots triggered spontaneous nodule formation, with ~ 21% of transgenic plants forming nodules (Fig. 6A–H). Toluidine blue staining of nodule sections indicated an absence of rhizobia inside the spontaneous nodules compared to rhizobia-induced nodules (Fig. 6I,J), demonstrating that nodule-like structures were induced by the transgene and not by an unwanted rhizobial contamination. A previous study has shown that the cytokinin receptor *MtCRE1* regulates nodule formation in a *NIN*-dependent manner in *M. truncatula* [19]. To further investigate the genetic relationship between *LjRRB12*, *LjLHK1*, and *LjNIN* in *L. japonicus*, we compared the spontaneous nodulation induced by LjRRB12^{D76E} in the roots of *hit1* and *nin2*. Expression of LjRRB12^{D76E} in *hit1* roots resulted in spontaneous nodule formation at a ratio of ~ 12%, whereas no spontaneous nodules formed in *nin2* roots (Fig. 6K–N). These results indicate that *LjRRB12* functions downstream of *LjLHK1* and upstream of *LjNIN*.

We performed a quantitative real-time PCR analysis to compare the transcriptional response of nodulation-related genes in spontaneous nodules. The expression of early nodulation genes, including *LjNIN*, *LjNF-YA1*, *LjNSP2*, and *LjERN1*, was upregulated in spontaneous nodules (Fig. 6O and Additional file 1: Fig. S6A), indicating that LjRRB12^{D76E} is sufficient to activate nodulation signaling. Interestingly, *LjCLE-RS3* showed a trend for a higher transcript abundance in spontaneous nodules, although the difference was not statistically significant (Additional file 1: Fig. S6B). Many of the cytokinin signaling genes, including *LjRRB12*, *LjRRA3*, *LjLHK1*, *LjRRA5*, and *LjIPT3*, were upregulated in spontaneous nodules (Fig. 6P and Additional file 1: Fig. S6C-E). In contrast, two cell cycle switch-related genes, *LjCCS52A1* and *LjCCS52A1-like2*, were either unchanged or repressed in the spontaneous nodules (Additional file 1: Fig. S6F-G). Taken together, these results indicate that ectopic expression of LjRRB12^{D76E} could trigger spontaneous nodule formation by activating the expression of early nodulation and the cytokinin signaling-related genes.

Discussion

In this study, we characterized a Type-B response regulator, *LjRRB12,* which acts as a regulator of nodule formation by activating the expression of *LjNIN*. We observed an increase in the number of eITs and a reduced number of nodule primordia in mutants with insertions in *LjRRB12* (Fig. 3K, L) and that constitutive expression of *LjRRB12* and its gain-of-function variant *LjRRB12*^{D76E} induced the formation of spontaneous nodules in the absence of rhizobia (Fig. 6A–N). LjRRB12 interacts with remote regions of the *LjNIN* promoter (Fig. 5C–F) and contributes to cytokinin-induced *LjNIN* expression (Fig. 5B). We conclude that LjRRB12 mediates crosstalk between cytokinin signaling and symbiotic signaling to regulate nodulation.

Expressions of *LjNIN* and *LjRRB12* were localized to the same root cells during the early stages of rhizobial infection (Fig. 2D–F, I, J and Additional file 1: Fig. S5A-C). This co-localized pattern of expression during the early stage of infection is consistent with a possible direct interaction occurring in planta that leads to the division of cortical cells and the development of nodule primordia after rhizobial infection. Notably, the expression of

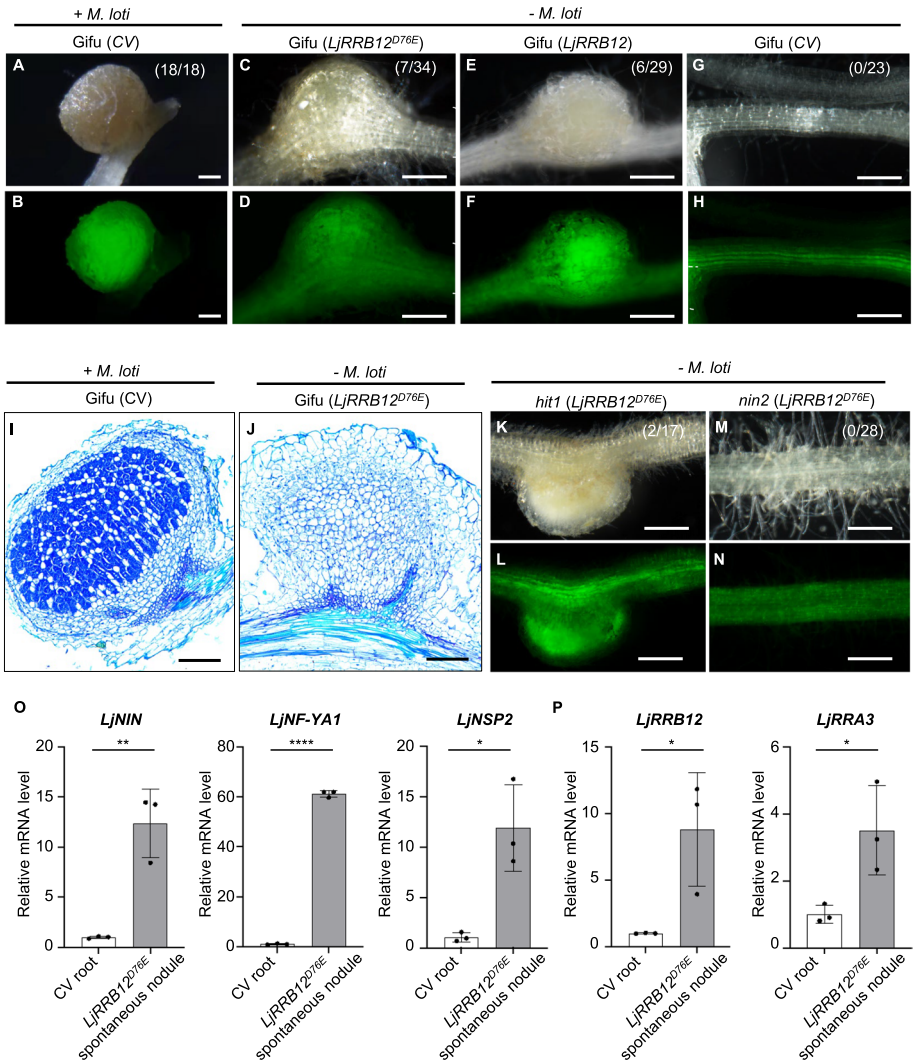

Fig. 6 Overexpression of *LjRRB12* triggers spontaneous nodule formation. Roots of Gifu, *hit1* and *nin2* transiently expressing the control vector *LjUBQ1::StrepII* (**A**, **B**, **G**, **H**), *LjUBQ1::LjRRB12* (**E**,**F**), or *LjUBQ1::LjRRB12*^{D76E} (**C**, **D**, **K**–**N**) were inoculated with (+*M. loti*) or without (−*M. loti*) rhizobia. Images were taken at 5 weeks after inoculation. Spontaneous nodules were formed in Gifu expressing *LjRRB12* (**E**, **F**) or the gain-of-function variant *RRB12*^{D76E} (**C**, **D**). The spontaneous nodule formation was also observed in *hit1* expressing *RRB12*^{D76E} (**K**, **L**), but not in *nin2* (**M**, **N**). Numbers in the upper right corners indicate the number of plants out of the total number of analyzed plants containing rhizobia-derived nodules or spontaneous nodules. Nodule sections in inoculated roots (**I**) and spontaneous nodule sections in uninoculated roots (**J**) were stained by toluidine blue. Scale bars, 100 μm (**I**, **J**) and 250 μm (**A**–**H, K**–**N**). **O**,**P** Transcript abundance of representative symbiotic signaling genes (*LjNIN*, *LjNF-YA1*, *LjNSP2*) (**O**) and cytokinin signaling genes (*LjRRB12*,*LjRRA3*) (**P**) in the spontaneous nodules of *LjUBQ1::LjRRB12*^{D76E} relative to the roots of *LjUBQ1::StrepII* (*CV*) in Gifu background. Values indicate means ± SD calculated from three biological replicates. A non-parametric test was used for statistical comparisons. *, $P < 0.05$; **, $P < 0.01$; ****, $P < 0.0001$

LjRRB12 in vascular bundles was heterogeneous (Fig. 2I). Similarly, the genes encoding the cytokinin receptor *LjLHK1* [29] and that contribute to the biosynthesis of cytokinin *MtIPT3* [65] were both expressed in the vascular bundle cells adjacent to the dividing cortical cells. Enhancing cytokinin activity in the vascular bundles may determine whether cells develop into nodules rather than into lateral roots by increasing the cytokinin/auxin ratio. As the nodules develop, the expression of *LjRRB12* is eventually localized only to vascular bundles (Fig. 2H, L). Loss of LjRRB12 function also leads to impaired nitrogen fixing activity in mature nodules (Fig. 4D–E).

Type-B RRs, a multigene family of transcription factors involved in cytokinin signaling, are the key components regulating the temporal and spatial development of plant responses to the cytokinin signal. Functional redundancy exists among RRBs in regulating non-symbiotic traits, especially in higher plants [55, 66]. Similarly, substantial

functional redundancy among RRBs in legumes is evident in their symbiotic effects. MtRRB1 and MtRRB3 in *M. truncatula* were reported to facilitate nodulation to varying degrees [35, 49]. In this study, the insertional mutations in *LjRRB12* resulted in a weakly reduced number of nodule primordia, which provides evidence for redundancy with other members of the *LjRRB* family. In agreement with this hypothesis, activation of *LjNIN* expression in response to cytokinin in the *ljrrb12-1* mutant was not completely suppressed, possibly due to other RRBs (Fig. 5B).

At an early stage of symbiosis, the symbiotic signal transduced by *LjNFR1*/*LjNFR5* and *LjSYMRK*/*MtDMI2* induces calcium spiking, which is essential for the progression of epidermal infection [5, 67–69]. However, calcium spiking is restricted to epidermal cells at a distance from the outer cortical cells [19, 70]. The mechanism that activates cortical cell divisions remains poorly understood. Cytokinin could be the signal that moves from the epidermis to cortex. *ITP2* and *IPT4* contribute to cytokinin biosynthesis. Their expression is induced in the epidermis, and the cytokinin response element *TCSn* is active mainly in root cortex [27]. Genetic studies indicate that nodule initiation depends on the expression of *LjLHK1*/*MtCRE1* [30, 71, 72], *NSP2* [36], *DELLAs* [73], and *NIN* [19] in the cortex. The decreased number of nodule primordia and mature nodules in the *ljrrb12* mutants (Fig. 3L and Fig. 4C) indicates a possible role for LjRRB12 in nodule organogenesis. Spontaneous nodule-like structures or bumps were observed in the gain-of-function mutants of *LjCCaMK* (*snf1*) [74], *LjLHK1* (*snf2*) [36], and in transgenic roots overexpressing *MtNIN* [19]. We discovered that the ubiquitin promoter (*LjUBQ1*) driving the expression of *LjRRB12* and its active form variant *LjRRB12*^{D76E} induced spontaneous nodules in *L. japonicus* roots in the absence of rhizobia (Fig. 6C–F, J), indicating that LjRRB12 and LjRRB12^{D76E} efficiently mimic NF-induced nodulation signaling and indicating a possible role for LjRRB12 in root nodule organogenesis. Additionally, LjRRB12^{D76E} induced spontaneous nodule formation on *hit1* roots (Fig. 6K–L), indicating that LjRRB12^{D76E}-mediated signaling functions probably downstream of LjLHK1. In contrast, nodule-like structures were not observed in *nin2* roots (Fig. 6M–N). This corroborates previous studies showing that cytokinin signal functions upstream of *LjNIN*-dependent nodulation signaling [75]. In addition, overexpression of LjRRB12^{D76E} is sufficient to activate nodulation genes including *LjNIN*, *LjNF-YA1*, *LjNSP2*, and *LjERN1* (Fig. 6O and Additional file 1: Fig. S6A).

As a master regulator of the symbiosis, the expression of *NIN* requires fine spatiotemporal control [19]. Approximately 2.2 kb upstream of the translational start codon from the *MtNIN* gene was sufficient for inducing expression in the epidermis that is responsible for root hair curling and establishment of infection chambers [33]. The − 5 to − 2.2 kb promoter region of *MtNIN*, containing a putative CYCLOPS binding site, is required for an effective IT formation [33]. A distant *cis*-element in the *MtNIN* promoter, called the cytokinin response element (CE), was shown in *M. truncatula* to mediate the cytokinin-regulated pericycle and cortical expression of *MtNIN* [33]. It is predicted that the D1 and D3 regions of the CE element contain several binding sites for RRBs, which provides evidence that the *MtNIN* gene is a direct target of RRBs [33]. The *pMtNIN_D1* region could mediate the *NIN* expression that promotes nodule formation in the *M. truncatula daphne-like* mutant [33], indicating a significant contribution to nodulation for the *pMtNIN_D1* region. The *pMtNIN_D3* region partially contributed to the nodulation function of *NIN* in the cortex [33]. Sequence analysis indicates that CE/Region 2 of the *L. japonicus* NIN promoter also contains putative RRB binding sites (Additional file 1: Fig. S3A; Fig. 5C). The role of the *pLjNIN_D1* from CE/Region2 as a cytokinin-related region has not been previously described and awaits experimental validation. We showed that LjRRB12 interacts with the *pLjNIN_D1* and *pLjNIN_D3* regions in vitro and in vivo during nodulation (Fig. 5C–F). Overall, our study revealed an in vivo regulatory relationship between cytokinin signaling and symbiotic nodule formation.

The *ljrrb12* mutants formed a significantly increased number of eITs and a reduced number of nodule primordia and mature nodules (Fig. 3K, L and Fig. 4C), as previously described for the *hit1* (a loss-of-function mutant of *LjLHK1*) and *daphne* mutants (a weak *nin* mutant allele) [30, 75]. This could be related to an attenuated inhibitory signal initiated in the root cortex, as the epidermal expression of *LjLHK1* could not reduce the *ljlhk1* hyper-infection events [72]. Previous research showed that LjNIN inhibits hyper-infection events by inducing *LjCLE-RS1/2* expression, which activates a shoot–root regulation of infections in an LjHAR1 (HYPERNODULATION AND ABERRANT ROOT FORMATION 1)-dependent manner [59]. Our study found that cytokinin upregulated the transcript abundance of *LjCLE-RS1/2/3* and that deficiency of LjRRB12 inhibited or even abolished the upregulated expression of these genes (Additional file 1: Fig. S2). Such reduction of *LjCLE-RS* gene expression in the *ljrrb12-1* mutant roots might promote the hyper-infection events, as evidenced by the enhanced eITs (Fig. 3K). Additionally, successful rhizobial infection requires the penetration of the root cortical cell wall [9]. Most infection threads of the *ljrrb12* mutants terminated at the root hair cells (Fig. 3G) with partial misorientation (Fig. 3I)

and resulted in a lower number of cITs and nodule primordia (Fig. 3K, L). The mechanism underlying cytokinin signaling and regulation of infection thread orientation, such as callose deposition [76] and pectate lyase activity [8], requires further investigation.

It is worth noting that nodule-like structures induced by cytokinin are restricted to legume plants [63]. The CE element exists in the promoters of *NIN* genes from legumes but is absent from both legume and non-legume *NLP* genes (Fig. 5C and Additional file 1: Fig. S3A) [61]. In *A. thaliana*, the GRAS proteins, GAI and RGA, interact with and enhance the transcriptional activity of ARR1 [77]. Several GRAS family proteins, including NSP1, NSP2, and DELLA, are direct or indirect positive regulators of *NIN* during nodule organogenesis [12, 78–81]. Whether there is cross-talk involving LjRRB12 and other regulators that fine-tunes *NIN* expression is an interesting question to be explored in the future.

Conclusions

Our study revealed the symbiotic functions of a B-type RR gene, *LjRRB12*, during an early stage of rhizobial infection and following nodule development. Our data highlight a negative role of LjRRB12 in regulating epidermal infection but a positive role in promoting nodulation. LjRRB12 regulates *LjNIN* expression by binding the *cis*-elements of the distal *LjNIN* promoter region, and LjRRB12 induces spontaneous nodule formation in the absence of rhizobia by acting upstream of LjNIN. These observations indicate that the cross talk between cytokinin signaling and symbiotic signaling is essential for proper rhizobial infection and subsequent nodule organogenesis.

Methods

Plant materials and growth conditions

Lotus japonicus Gifu, *nin-2* [18] and *hit1* [30] mutants were used in this study. The *ljrrb12-1* (Plant ID: 30146471) and *ljrrb12-2* (Plant ID: 30015963) mutants were obtained from the *LORE1* (*Lotus Retrotransposon 1*) mutant resource (https://lotus.au.dk) [51, 57]. *L. japonicus* seeds were scarified with sulfuric acid for 6 min and surface sterilized with 2% sodium hypochlorite for 8 min. After 1 day of vernalization at 4°C in the dark, the seeds were dispersed onto half-strength Murashige–Skoog (MS) agar plates. Then the seeds were germinated in a growth chamber for 2 days in the dark and 3 days in the light at 23°C with a photoperiod containing 16 h light and 8 h of dark and light fluence rate of *c.* 120 μmol photons m^{-2} s^{-1}. For the symbiotic phenotype analysis, germinated seeds were grown in sterilized vermiculite-perlite for 5 days before inoculation with *Mesorhizobium loti* MAFF303099. Plants were cultivated with half-strength B&D solution containing 0.5 mM KNO_3 [82]. For cytokinin treatment, plants grown in vermiculite-perlite for 7 days were washed and then incubated with half-strength B&D nutrient solution containing 10^{-7} M 6-BA for 1 h at room temperature.

Histochemical staining

For promoter expression analysis, a 3-kb promoter region of *LjRRB12* and a 5-kb promoter region with the additional CE element (−43209 to −43759 bp upstream of translational start site) of *LjNIN* were amplified from Gifu genomic DNA and cloned upstream of the *GUS* reporter gene in the DX2181G-GUS vector. The constructed plasmids were introduced into *L. japonicus* roots using *Agrobacterium rhizogenes* strain LBA1334 as described previously [83]. The hairy roots were inoculated with *M. loti* MAFF303099 and harvested at 0, 3, 5, 7, 14, and 21 dpi. The hairy roots were fixed with cold 90% (v/v) acetone and stained for GUS activity using 0.5 mg/ml 5-bromo-4-chloro-3-indolyl-β-D-glucuronic acid cyclohexylammonium salt (Sangon Biotech, A610085), 10 mM EDTA, 1 mM potassium hexacyanoferrate (II), 1 mM potassium hexacyanoferrate (III), 0.1% N-Lauroylsarcosine sodium salt, 0.1% (v/v) Triton X-100, and 50 mM sodium phosphate (pH 7.0). All tissues were stained overnight in vacuum at room temperature and washed sequentially with 70% alcohol and chloral hydrate solution (chloral hydrate: water: glycerol, 10:3:2, w/v/v). The stained roots and nodules were embedded in the 4% agarose and then sectioned (root, 50 μm; nodule, 70 μm) using a VT1000S vibratome (Leica, Germany). Images of sectioned samples were captured using a Leica DM2500 microscope (Leica, Germany).

Sequence alignment and phylogenetic analysis

The amino acid sequences of RRBs from *L. japonicus* were obtained from the Lotus base Gifu version 1.3 using BLAST searches (Additional File 2: Table S1) [50, 51] with the *A. thaliana* ARR1 (Gene ID: AT3G16857) and ARR2 (Gene ID: AT4G16110) amino acid sequences retrieved from TAIR [84]. The RRB sequences from *L. japonicus* MG20 obtained from MG20 V3.0 [85] were also used for annotation corrections. RRB sequences from *M. truncatula* were selected using BLAST searches of the *M. truncatula* Mt4.0v1 genome from Phytozome v13 [86, 87]. Amino acid sequences were aligned using DNAMAN 10. A phylogenetic tree was constructed in MEGA 11 using a Neighbor-Joining method and 1000 bootstrap replicates.

For *NIN* promoter analysis, promoter sequences of *NIN* from *L. japonicus*, *Arachis hypogaea*, *Trifolium pretense*, *Cicer arietinum*, *Glycine max*, *Medicago*

truncatula, *Lupinus albus*, and *LjNLP1-5* of *L. japonicus* were retrieved from Phytozome v13 [86]. The ~ 50-kb promoter sequences upstream of the start codon were aligned in mVISTA [88] using the Shuffle-LAGAN mode [89].

Acetylene reduction assay

Acetylene reduction assays were performed in sealed glass bottles. The nodulated roots from five plants were placed into a reaction bottle and 4 ~ 6 biological replicates were analyzed. Acetylene (2 ml) was added to the bottles and incubated at 28 °C for 2 h. GC-4000A gas chromatography (East &West Analytical Instruments, China) was used to quantify ethylene production.

Spontaneous formation of nodule-like structures on hairy roots

The full-length coding sequence of *LjRRB12* was amplified from an *L. japonicus* Gifu cDNA library and inserted into *pUB-GFP* [90] to produce the *pUB-GFP-pLjUBQ1::LjRRB12* plasmid. To construct the phosphomimetic LjRRB12^{D76E} vector, we introduced a T to A substitution with primer pairs LjRRB12-F/LjRRB12-D76E-R and LjRRB12-D76E-F/LjRRB12-R. The mutated fragment of *LjRRB12* (LjRRB12^{D76E}) was cloned into *pUB-GFP* using the ClonExpress II One Step Cloning Kit (Vazyme, Nanjing, China) to generate *pUB-GFP-pLjUBQ1::LjRRB12^{D76E}*. The hairy roots of *hit1* and *nin-2* mutants from Gifu were respectively transformed with these constructs using *Agrobacterium rhizogenes* LBA1334. Plants with GFP-positive hairy roots were grown in sterilized vermiculite-perlite (2:1).

RT-PCR and qPCR

L. japonicus roots were harvested and immediately frozen in liquid nitrogen. Total RNA was extracted using the Transzol Plant kit (Transgene, ET121-01) and genomic DNA contamination was completely removed using RNase-free DNase I (ThermoFisher, EN0521). One microgram of total RNA was reverse transcribed using Reverse Transcriptase M-MLV (Thermo Fisher Scientific) with random hexamers. Quantitative RT-PCR was performed using a QuantStudio 5 Real-Time PCR System (Thermo Fisher Scientific) and the TransStart Tip Green qPCR SuperMix (Transgene, AQ141-01). *L. japonicus LjUBQ1* (GenBank accession no. AW720576) was used as a reference gene for calculating fold changes in relative expression using the $2^{-\Delta\Delta Ct}$ method. Primers used for RT-qPCR are provided in Additional File 3: Table S2.

The in vivo binding assay by nCUT&Tag-qPCR

The nCUT&Tag experiment was conducted following an established protocol with modifications using the Hieff NGS® G-Type In-Situ DNA Binding Profiling Library Prep Kit from Illumina (Yeasen, Shanghai, China). The vectors expressing 3 × Flag (EV) or LjRRB12-3 × Flag were induced into Gifu using a hairy root transformation procedure. The transgenic plants inoculated with *M. loti* MAFF333099 and the roots at 7 dpi were harvested. ~ 0.2 g of root tissue was immersed in formaldehyde fixing solution (10 mM Tris, pH 8.0, 10 mM KCl, 0.5 mM spermidine, 0.5% formaldehyde) for 5 min at room temperature. After adding 1 mL of 2 M glycine to stop the fixation, the root tissue was washed three times with 50 mL of ddH_2O and was rapidly frozen in liquid nitrogen for 2 min. After grinding, the cell pellets were resuspended in nuclear extraction buffer A (10 mM Tris–HCl, pH 8.0, 10 mM KCl, 0.5 mM spermidine), and the solution was filtered through a 40-μm filter. After discarding the supernatant, the pellet was washed with nuclear extraction buffer B (0.25 M sucrose, 10 mM Tris–HCl, pH 8.0, 10 mM $MgCl_2$, 1% Triton X-100, 5 mM β-mercaptoethanol, 0.1% Protease Inhibitor Cocktail) and subsequently with nuclear extraction buffer C (1.8 M sucrose, 10 mM Tris–HCl, pH 8.0, 2 mM $MgCl_2$, 0.15% Triton X-100, 5 mM β-mercaptoethanol, 0.1% Protease Inhibitor Cocktail). After centrifugation at 12,000 × *g* for 45 min at 4 °C, the nuclei from the root tissue were obtained and stained with trypan blue to detect their integrity using a Leica DM2500 microscope (Leica, Germany). Subsequently, nuclei were resuspended in nuclear extraction buffer D (10 mM Tris–HCl, pH 8.0, 150 mM NaCl, 0.5 mM spermidine, 0.1% Protease Inhibitor Cocktail). The following procedures were performed according to the previously described protocol [91]. qPCR procedures were performed using the manufacturer's instructions from the PerfectStart® Uni RT&qPCR Kit (Transgen Biotech, Beijing, China). nCUT&Tag-qPCR experiments were performed with two biological replicates with three technical repeats for each sample.

Electrophoretic mobility shift assay (EMSA)

To construct the GST-LjRRB12_BD expression vector, the coding region of LjRRB12 (aa 175–307) was amplified and inserted into *pGEX-6P1*. The expression of the GST-LjRRB12_BD fusion protein was induced using 0.3 mM IPTG in *Escherichia coli* BL21(DE3) and purified using glutathione resin (GenScript, L00206). Purified protein was dialyzed and then concentrated with an Amicon® Ultra-15 Centrifugal Filter (Millipore, UFC905008).

For DNA preparation, the *pGreenII-0800-NIN_D1-35Smini::LUC* and *pGreenII-0800-NIN_D1mut-35Smini::LUC* vectors were used as templates. To generate the *pGreenII-0800-NIN_D1-35Smini::LUC*, an NIN_D1 fragment and the CaMV35S minimal promoter (35Smin) fragment were fused to the *pGreenII-0800*

vector [92]. To generate *pGreenII-0800-NIN_D1mut-35Smini::LUC*, a synthesized mutant D1 sequence and 35Smin were fused in the *pGreenII-0800* vector. For D1 DNA probe preparation, a short NIN_D1 (WT sD1) fragment or a short NIN_D1mut (Mut sD1) fragment was amplified from *pGreenII-0800-NIN_D1-35Smini::LUC* or *pGreenII-0800-NIN_D1mut-35Smini::LUC* using the D1-S-F and 35Smini-R primers (the latter primer was either labeled or unlabeled with 5′ FAM). For the D3 DNA probe, 5′ FAM labeled and unlabeled DNA was synthesized by Sangon Biotech (Shanghai, China). EMSA was performed in 10 μL binding buffer containing 1 mM $MgCl_2$, 0.5 mM EDTA, 1 mM DTT, 0.5% Triton X-100, 25 ng/mL poly (dI, dC), 5% glycerol and 20 mM Tris–HCl, pH 8.0. The FAM-labeled probes were added at a molar mass of 0.5 pmol for D1 and 0.05 pmol for D3. GST and GST-LjRRB12_BD proteins were added at a 15-fold molar excess of the labeled D1 probe and at a 75-fold molar excess of the labeled D3 probe. The cold probe and mutant cold probe were added to the reaction tubes at a 5-, 20-, and 40-fold molar excess of FAM probe for D1 and at a 20-fold molar excess for D3. Mixtures were incubated at 25 °C for 20 min and then loaded onto 5% polyacrylamide gels with 0.5 × TBE running buffer (45 mM Tris–Borate, 1 mM EDTA) for electrophoresis. The signal of the FAM-labeled DNA was visualized with FLA-5100 Fluorescent Laser Analyzer (Fuji Film, Japan).

Systematic evolution of ligands by exponential enrichment (SELEX)

The SELEX experiment was based on a published protocol [93] with minor modifications. The GST-LjRRB12_BD protein was purified as described for the EMSA. A 51-bp double-stranded oligonucleotide library including a flanking connector and 12-bp random central core sequence [5′-GATGAAGCTTCCTGGACAAT(12N) GCAGTCACTGAAGAATTCT-3′] as described in [49] was amplified using PCR and purified using silicon dioxide (Sigma, S5631). The selection was performed for eight rounds. Each round of selection was performed in 500 μl of RSDA buffer (5 mM Tris–HCl, pH 8.0, 75 mM NaCl, 2.5 mM $MgCl_2$, 0.5 mM EDTA, 5% glycerol, 1% Tween 20, and 1 mM DTT) with 10 μg of purified DNA, smaller amounts of protein in each round (i.e., 25 μg, 22.5 μg, 21.5 μg, 20 μg, 18.75 μg, 17.5 μg, and 16.25 μg), increasing amounts of poly(dIdC) served as a non-specific competitor (i.e., 0, 200, 400, 600, 800, 1000, 1200, and 1400 ng), and 100 μL of glutathione resin (GenScript, L00206). The reaction components were incubated at 4 °C for 2 h and then washed four times with RSDA buffer. Beads were then mixed with 500 μL of ddH_2O and boiled for 10 min to release the bound DNA. Purification of the bound DNA was carried out using chloroform:isoamyl alcohol (24:1). Subsequently, the purified DNA was employed as a template in the PCR reaction for the preparation of the next round random DNA. PCR products were purified using glass microspheres. After eight rounds of selection, the oligonucleotides were cloned into pEASY-Blunt (Transgene, CB101-01) for sequencing. Forty-seven bacterial colonies were selected and twenty-nine non-repetitive sequences were used for the core motif analysis in MEME (https://meme-suite.org/meme/tools/meme) [62].

Statistical analysis

A non-parametric test ($n < 30$) and Student's t test ($n \geq 30$) were used for comparison of two groups. One-way ANOVA analysis and Tukey's multiple comparison tests were used to determine statistical significances among multiple groups.

Abbreviations

RRB	Type-B RESPONSE REGULATOR
ITs	Infection threads
CE	Cytokinin Response Element
NFs	Nodulation factors
TCS	Two-Component Signaling Sensor
RR	Response Regulator
HP	His-containing Phosphotransferase
bHLH	Basic Helix-Loop-Helix
NP	Nodule Primordium
6-BA	6-Benzylaminopurine
CYC-RE	CYCLOPS Response Element
LjNLP	*Lotus japonicus* NIN-like protein
SELEX	Systematic Evolution of Ligands by Exponential Enrichment
EMSA	Electrophoretic Mobility Shift Assay
AON	Autoregulation of nodule numbers
WT	Wild type
HZ	Heterozygous mutant
HM	Homozygous mutant
eIT	Epidermal infection thread
cIT	Cortical infection thread
FW	Fresh weight
snf2	Spontaneous nodule formation 2
hit1	Hyperinfected 1/lotus histidine kinase 1
nin2	Nodule inception 2
BD	Binding domain

Supplementary Information

The online version contains supplementary material available at https://doi.org/10.1186/s12915-024-02088-5.

Additional file 1: Fig. S1 Amino acid sequence alignment of *L. japonicus* RRBs and *A. thaliana* ARR1.Amino acid sequence alignment of the receiver domain (**A**) and DNA-binding domain (**B**) of *A. thaliana* ARR1 (AT3G16857.1) and RRBs of *L. japonicus*Gifu. Conserved amino acids (100% identity) are shadowed in black. Less conserved amino acids (>75% and <100%) are marked in gray. Amino acids essential for the phosphorelay in *A. thaliana* ARR1 are indicated with asterisks (D44, D89, K138). Fig. S2 Expression analysis of *L. japonicus CLE-RSs* after the cytokinin treatment. Expression analysis of *CLAVATA3/EMBRYO SURROUNDING REGION* (*CLE*)-related small peptide coding genes, including *LjCLE-RS1*, *LjCLE-RS2* and *LjCLE-RS3* in Gifu and *ljrrb12-1* roots after the treatment with 10^{-7} M 6-BA for 1 h. Relative mRNA levels were normalized against the *LjUBQ1* gene. Ctrl, Control. Data indicate mean values ± SD calculated from three biological replicates. Statistical analysis was performed using Tukey's

multiple comparison test. Means denoted by the same letter are not significantly different ($P < 0.05$). Fig. S3 Conservation of the CE region in the promoters of legume *NINs*.Alignment of genomic DNA sequences ~50 kb upstream of the translational start codon of *NIN* from seven legume species, including *Lotus japonicus*, *Arachis hypogaea*, *Trifolium pretense*, *Cicer arietinum*, *Glycine max*, *Medicago truncatula* and *Lupinus albus*. *LjNLP1-5* from *L. japonicus* were also included for comparison. The alignment was performed using mVISTA. Peaks denote identity levels higher than 50% per 100 bp relative to *LjNIN*. The ruler scales correspond to base numbers relative to the translational start site. Black arrows denote the conserved region. (**B**) List of *NIN* and*NLP* genes used in (**A**). Fig. S4 SELEX identification of the consensus sequence bound by LjRRB12.(**A**) Consensus sequence identified after eight rounds of selection using SELEX (Systematic Evolution of Ligands by EXponential enrichment). The SELEX motif 5′-(A/T)GAT(A/T)(C/T)-3′ identified from *L. japonicus* is quite similar to the Arabidopsis 6-bp RRB binding motif, which also contains the core motif "AGAT". The Medicago RRB binding motif also includes the core sequence "AGA" but is more variable at the remaining sites. (**B**) Sequence alignment was performed in MEME and the consensus sequence was generated. (**C**) WT sD1, Mut sD1, WT sD3 and Mut sD3 sequences used for the EMSA in (Fig. 5E-F). The LjRRB12 putative binding sites are highlighted blue in WT sD1 and WT sD3, and mutated sequences are highlighted red in Mut sD1 and Mut sD3. Fig. S5 Analysis of *CE-NIN*$_{5K}$ promoter activity at different stages of nodule development. Promoter activity was assayed by staining for GUS activity in transgenic hairy roots harboring *CE-NIN*$_{5K}$::GUS at different stages of nodule development, including in nodule primordia at 3 and 5 dpi (**A**,**B**), young nodules at 7 and 14 dpi (**C**,**D**), and mature nodules at 21 dpi (**E**). In (**A**), black and white arrows respectively indicate the root cortical and epidermal cells expressing *GUS*. Images are representative of at least ten independent transgenic plants. Scale bars, 100 μm (**A**, **C**), and 200 μm (**B**, **D**, **E**). *CE-NIN*$_{5K}$, a promoter fusion including a ~5-kb promoter region upstream of the translation start site and the ~550 bp CE (cytokinin response element) region of *LjNIN* gene. VB, vascular bundle; NC, nodule cortex; NP, nodule primordium. Fig. S6 Representative gene expression changes in *LjRRB12*^{D76E}-triggered spontaneous nodules. Expression of the symbiotic signaling gene *LjERN1* (**A**), autoregulation of nodulation gene *LjCLE-RS3* (**B**), cytokinin signaling related genes *LjLHK1*, *LjRRA5*, and *LjIPT3* (**C**-**E**), and cell cycle switch related genes, *LjCCS52A1* and *LjCCS52A1-like2* (**F**,**G**) in the *LjUBQ1*::*LjRRB12*^{D76E}-derived spontaneous nodules relative to the roots of control vector (CV) expressing *LjUBQ1*::*StrepII*. Values indicate means ± SD calculated from two or three biological replicates. A non-parametric test was used for statistical comparisons. ns, not significant; *, $P < 0.05$; **,$P < 0.01$.

Additional file 2: Table S1. List of genes found in the genome of *L. japonicus*.

Additional file 3: Table S2. Primers used in this study.

Additional file 4: Original images for Fig. 3B and Fig. 5E-F.

Acknowledgements
We thank the Lotus Base for providing the ljrrb12 mutant seeds. We thank Professor Robert M Larkin (Huazhong Agricultural University) for reading and editing the manuscript.

Authors' contributions
JC, YZ, JJ, LW1, LW2, and DD designed the research. JC, YZ, TT, JJ, YD, YG, YQ, and YH performed the experiments. JC, YZ, TT, JJ, QF, and DD analyzed the data. JC, YZ, JJ, and DD wrote the manuscript. JC, YZ, TT, and JJ contributed equally to this work. All authors read and approved the final manuscript.

Funding
This work was supported by National Natural Science Foundation of China (31870220), the Foundation of Hubei Hongshan Laboratory (2022hszd014), HZAU-AGIS Cooperation Fund (SZYJY2022005), Anhui Provincial Natural Science Foundation (2308085QC75), and Major Natural Science Foundation of the Anhui Educational Committee (2023AH052250).

Data availability
All data generated or analyzed in this study are included in this published article and its supplementary information files.

Declarations

Ethics approval and consent to participate
Not applicable.

Consent for publication
Not applicable.

Competing interests
The authors declare that they have no competing interests.

Received: 20 December 2023 Accepted: 2 December 2024
Published online: 18 December 2024

References

1. Redmond JW, Batley M, Djordjevic MA, Innes RW, Kuempel PL, Rolfe BG. Flavones induce expression of nodulation genes in Rhizobium. Nature. 1986;323:632–5.
2. Peters NK, Frost JW, Long SR. A plant Flavone, Luteolin, induces expression of Rhizobium-Meliloti nodulation genes. Science. 1986;233:977–80.
3. Denarie J, Debelle F, Prome JC. Rhizobium lipo-chitooligosaccharide nodulation factors: signaling molecules mediating recognition and morphogenesis. Annu Rev Biochem. 1996;65:503–35.
4. van der Drift KM, Olsthoorn MM, Brull LP, Blok-Tip L, Thomas-Oates JE. Mass spectrometric analysis of lipo-chitin oligosaccharides–signal molecules mediating the host-specific legume-rhizobium symbiosis. Mass Spectrom Rev. 1998;17:75–95.
5. Sieberer BJ, Chabaud M, Timmers AC, Monin A, Fournier J, Barker DG. A nuclear-targeted cameleon demonstrates intranuclear Ca2+ spiking in Medicago truncatula root hairs in response to rhizobial nodulation factors. Plant Physiol. 2009;151:1197–206.
6. Kelner A, Leitao N, Chabaud M, Charpentier M, de Carvalho-Niebel F. Dual color sensors for simultaneous analysis of calcium signal dynamics in the nuclear and cytoplasmic compartments of plant cells. Front Plant Sci. 2018;9:245.
7. Crdenas L, Vidali L, Domnguez J, Prez H, Snchez F, Hepler PK, Quinto C. Rearrangement of actin microfilaments in plant root hairs responding to rhizobium etli nodulation signals. Plant Physiol. 1998;116:871–7.
8. Xie F, Murray JD, Kim J, Heckmann AB, Edwards A, Oldroyd GED, Downie A. Legume pectate lyase required for root infection by rhizobia. Proc Natl Acad Sci U S A. 2012;109:633–8.
9. Roy S, Liu W, Nandety RS, Crook A, Mysore KS, Pislariu CI, Frugoli J, Dickstein R, Udvardi MK. Celebrating 20 years of genetic discoveries in legume nodulation and symbiotic nitrogen fixation. Plant Cell. 2020;32:15–41.
10. Singh S, Parniske M. Activation of calcium- and calmodulin-dependent protein kinase (CCaMK), the central regulator of plant root endosymbiosis. Curr Opin Plant Biol. 2012;15:444–53.
11. Yano K, Yoshida S, Muller J, Singh S, Banba M, Vickers K, Markmann K, White C, Schuller B, Sato S, et al. CYCLOPS, a mediator of symbiotic intracellular accommodation. Proc Natl Acad Sci U S A. 2008;105:20540–5.
12. Singh S, Katzer K, Lambert J, Cerri M, Parniske M. CYCLOPS, A DNA-binding transcriptional activator, orchestrates symbiotic root nodule development. Cell Host Microbe. 2014;15:139–52.
13. Middleton PH, Jakab J, Penmetsa RV, Starker CG, Doll J, Kalo P, Prabhu R, Marsh JF, Mitra RM, Kereszt A, et al. An ERF transcription factor in Medicago truncatula that is essential for Nod factor signal transduction. Plant Cell. 2007;19:1221–34.
14. Liu M, Soyano T, Yano K, Hayashi M, Kawaguchi M. ERN1 and CYCLOPS coordinately activate NIN signaling to promote infection thread formation in Lotus japonicus. J Plant Res. 2019;132:641–53.

15. Oldroyd GE, Long SR. Identification and characterization of nodulation-signaling pathway 2, a gene of Medicago truncatula involved in Nod actor signaling. Plant Physiol. 2003;131:1027–32.
16. Kalo P, Gleason C, Edwards A, Marsh J, Mitra RM, Hirsch S, Jakab J, Sims S, Long SR, Rogers J, et al. Nodulation signaling in legumes requires NSP2, a member of the GRAS family of transcriptional regulators. Science. 2005;308:1786–9.
17. Smit P, Raedts J, Portyanko V, Debelle F, Gough C, Bisseling T, Geurts R. NSP1 of the GRAS protein family is essential for rhizobial Nod factor-induced transcription. Science. 2005;308:1789–91.
18. Schauser L, Roussis A, Stiller J, Stougaard J. A plant regulator controlling development of symbiotic root nodules. Nature. 1999;402:191–5.
19. Vernie T, Kim J, Frances L, Ding YL, Sun J, Guan D, Niebel A, Gifford ML, de Carvalho-Niebel F, Oldroyd GED. The NIN Transcription factor coordinates diverse nodulation programs in different tissues of the Medicago truncatula Root. Plant Cell. 2015;27:3410–24.
20. Liu CW, Breakspear A, Guan D, Cerri MR, Jackson K, Jiang SY, Robson F, Radhakrishnan GV, Roy S, Bone C, et al. NIN Acts as a network hub controlling a growth module required for rhizobial infection. Plant Physiol. 2019;179:1704–22.
21. Dong W, Zhu Y, Chang H, Wang C, Yang J, Shi J, Gao J, Yang W, Lan L, Wang Y, et al. An SHR-SCR module specifies legume cortical cell fate to enable nodulation. Nature. 2021;589:586–90.
22. Rolfe BG, Gresshoff PM. Genetic-analysis of Legume Nodule initiation. Annu Rev Plant Physiol Plant Mol Biol. 1988;39:297–319.
23. van Spronsen PC, Gronlund M, Bras CP, Spaink HP, Kijne JW. Cell biological changes of outer cortical root cells in early determinate nodulation. Mol Plant Microbe Interact. 2001;14:839–47.
24. Oldroyd GE, Murray JD, Poole PS, Downie JA. The rules of engagement in the legume-rhizobial symbiosis. Annu Rev Genet. 2011;45:119–44.
25. Lin J, Frank M, Reid D. No home without hormones: how plant hormones control legume nodule organogenesis. Plant Commun. 2020;1:100104.
26. van Zeijl A, den Camp RHMO, Deinum EE, Charnikhova T, Franssen H, den Camp HJMO, Bouwmeester H, Kohlen W, Bisseling T, Geurts R. Rhizobium lipo-chitooligosaccharide signaling triggers accumulation of cytokinins in Medicago truncatula roots. Mol Plant. 2015;8:1213–26.
27. Reid D, Nadzieja M, Novak O, Heckmann AB, Sandal N, Stougaard J. Cytokinin biosynthesis promotes cortical cell responses during nodule development. Plant Physiol. 2017;175:361–75.
28. Jarzyniak K, Banasiak J, Jamruszka T, Pawela A, Di Donato M, Novak O, Geisler M, Jasinski M. Early stages of legume-rhizobia symbiosis are controlled by ABCG-mediated transport of active cytokinins. Nat Plants. 2021;7:428–36.
29. Held M, Hou HW, Miri M, Huynh C, Ross L, Hossain MS, Sato S, Tabata S, Perry J, Wang TL, et al. Lotus japonicus Cytokinin Receptors Work Partially Redundantly to Mediate Nodule Formation. Plant Cell. 2014;26:678–94.
30. Murray JD, Karas BJ, Sato S, Tabata S, Amyot L, Szczyglowski K. A cytokinin perception mutant colonized by Rhizobium in the absence of nodule organogenesis. Science. 2007;315:101–4.
31. Heckmann AB, Sandal N, Bek AS, Madsen LH, Jurkiewicz A, Nielsen MW, Tirichine L, Stougaard J. Cytokinin Induction of Root Nodule Primordia in Lotus japonicus Is Regulated by a Mechanism Operating in the Root Cortex. Mol Plant Microbe. 2011;24:1385–95.
32. Plet J, Wasson A, Ariel F, Le Signor C, Baker D, Mathesius U, Crespi M, Frugier F. MtCRE1-dependent cytokinin signaling integrates bacterial and plant cues to coordinate symbiotic nodule organogenesis in Medicago truncatula. Plant J. 2011;65:622–33.
33. Liu JY, Rutten L, Limpens E, van der Molen T, van Velzen R, Chen RJ, Chen YH, Geurts R, Kohlen W, Kulikova O, et al. A Remote cis-Regulatory Region Is Required for NIN Expression in the Pericycle to Initiate Nodule Primordium Formation in Medicago truncatula. Plant Cell. 2019;31:68–83.
34. Schiessl K, Lilley JLS, Lee T, Tamvakis I, Kohlen W, Bailey PC, Thomas A, Luptak J, Ramakrishnan K, Carpenter MD, et al. NODULE INCEPTION recruits the lateral root developmental program for symbiotic nodule organogenesis in Medicago truncatula. Curr Biol. 2019;29:3657–68.
35. Tan S, Sanchez M, Laffont C, Boivin S, Le Signor C, Thompson R, Frugier F, Brault M. A cytokinin signaling Type-B response regulator transcription factor acting in early nodulation. Plant Physiol. 2020;183:1319–30.
36. Tirichine L, Sandal N, Madsen LH, Radutoiu S, Albrektsen AS, Sato S, Asamizu E, Tabata S, Stougaard J. A gain-of-function mutation in a cytokinin receptor triggers spontaneous root nodule organogenesis. Science. 2007;315:104–7.
37. Reid DE, Heckmann AB, Novak O, Kelly S, Stougaard J. CYTOKININ OXIDASE/DEHYDROGENASE3 Maintains Cytokinin Homeostasis during Root and Nodule Development in Lotus japonicus. Plant Physiol. 2016;170:1060–74.
38. Lin J, Roswanjaya YP, Kohlen W, Stougaard J, Reid D. Nitrate restricts nodule organogenesis through inhibition of cytokinin biosynthesis in Lotus japonicus. Nat Commun. 2021;12:6544.
39. Sauviac L, Remy A, Huault E, Dalmasso M, Kazmierczak T, Jardinaud MF, Legrand L, Moreau C, Ruiz B, Cazale AC, et al. A dual legume-rhizobium transcriptome of symbiotic nodule senescence reveals coordinated plant and bacterial responses. Plant Cell Environ. 2022;45:3100–21.
40. Gao R, Stock AM. Biological insights from structures of two-component proteins. Annu Rev Microbiol. 2009;63:133–54.
41. Hwang I, Sheen J. Two-component circuitry in Arabidopsis cytokinin signal transduction. Nature. 2001;413:383–9.
42. Yamada H, Suzuki T, Terada K, Takei K, Ishikawa K, Miwa K, Yamashino T, Mizuno T. The Arabidopsis AHK4 histidine kinase is a cytokinin-binding receptor that transduces cytokinin signals across the membrane. Plant Cell Physiol. 2001;42:1017–23.
43. Heyl A, Wulfetange K, Pils B, Nielsen N, Romanov GA, Schmulling T. Evolutionary proteomics identifies amino acids essential for ligand-binding of the cytokinin receptor CHASE domain. BMC Evol Biol. 2007;7:62.
44. Schaller GE, Doi K, Hwang I, Kieber JJ, Khurana JP, Kurata N, Mizuno T, Pareek A, Shiu SH, Wu P, et al. Nomenclature for two-component signaling elements of rice. Plant Physiol. 2007;143:555–7.
45. Heyl A, Brault M, Frugier F, Kuderova A, Lindner AC, Motyka V, Rashotte AM, von Schwartzenberg K, Vankova R, Schaller GE. Nomenclature for Members of the Two-Component Signaling Pathway of Plants. Plant Physiol. 2013;161:1063–5.
46. Sakai H, Aoyama T, Bono H, Oka A. Two-component response regulators from Arabidopsis thaliana contain a putative DNA-binding motif. Plant Cell Physiol. 1998;39:1232–9.
47. Argyros RD, Mathews DE, Chiang YH, Palmer CM, Thibault DM, Etheridge N, Argyros DA, Mason MG, Kieber JJ, Schaller GE. Type B response regulators of Arabidopsis play key roles in cytokinin signaling and plant development. Plant Cell. 2008;20:2102–16.
48. Kieber JJ, Schaller GE. Cytokinin signaling in plant development. Development. 2018;145(4):dev149344.
49. Ariel F, Brault-Hernandez M, Laffont C, Huault E, Brault M, Plet J, Moison M, Blanchet S, Ichante JL, Chabaud M, et al. Two direct targets of cytokinin signaling regulate symbiotic nodulation in Medicago truncatula. Plant Cell. 2012;24:3838–52.
50. Kamal N, Mun T, Reid D, Lin JS, Akyol TY, Sandal N, Asp T, Hirakawa H, Stougaard J, Mayer KFX, et al. Insights into the evolution of symbiosis gene copy number and distribution from a chromosome-scale Lotus japonicus Gifu genome sequence. DNA Res. 2020;27(3):dsaa015.
51. Mun T, Bachmann A, Gupta V, Stougaard J, Andersen SU. Lotus Base: An integrated information portal for the model legume Lotus japonicus. Sci Rep. 2016;6:39447.
52. Kaltenegger E, Leng S, Heyl A. The effects of repeated whole genome duplication events on the evolution of cytokinin signaling pathway. BMC Evol Biol. 2018;18(1):76.
53. Argueso CT, Raines T, Kieber JJ. Cytokinin signaling and transcriptional networks. Curr Opin Plant Biol. 2010;13:533–9.
54. Xie MT, Chen HY, Huang L, O'Neil RC, Shokhirev MN, Ecker JR. A B-ARR-mediated cytokinin transcriptional network directs hormone cross-regulation and shoot development. Nat Commun. 2018;9:2075.
55. Mason MG, Mathews DE, Argyros DA, Maxwell BB, Kieber JJ, Alonso JM, Ecker JR, Schaller GE. Multiple type-B response regulators mediate cytokinin signal transduction in Arabidopsis. Plant Cell. 2005;17:3007–18.
56. Tan S, Debelle F, Gamas P, Frugier F, Brault M. Diversification of cytokinin phosphotransfer signaling genes in Medicago truncatula and other legume genomes. BMC Genomics. 2019;20:373.
57. Malolepszy A, Mun T, Sandal N, Gupta V, Dubin M, Urbanski D, Shah N, Bachmann A, Fukai E, Hirakawa H, et al. The LORE1 insertion mutant resource. Plant J. 2016;88:306–17.
58. Kiba T, Taniguchi M, Imamura A, Ueguchi C, Mizuno T, Sugiyama T. Differential expression of genes for response regulators in response

to cytokinins and nitrate in Arabidopsis thaliana. Plant Cell Physiol. 1999;40:767–71.
59. Yoro E, Suzaki T, Kawaguchi M. CLE-HAR1 Systemic Signaling and NIN-Mediated Local Signaling Suppress the Increased Rhizobial Infection in the daphne Mutant of Lotus japonicus. Mol Plant Microbe Interact. 2020;33:320–7.
60. Fu M, Sun J, Li X, Guan Y, Xie F. Asymmetric redundancy of soybean Nodule Inception (NIN) genes in root nodule symbiosis. Plant Physiol. 2022;188:477–89.
61. Liu J, Bisseling T. Evolution of NIN and NIN-like Genes in Relation to Nodule Symbiosis. Genes (Basel). 2020;11:777.
62. Bailey TL, Boden M, Buske FA, Frith M, Grant CE, Clementi L, Ren J, Li WW, Noble WS. MEME SUITE: tools for motif discovery and searching. Nucleic Acids Res. 2009;37:W202-208.
63. Gauthier-Coles C, White RG, Mathesius U. Nodulating legumes are distinguished by a sensitivity to cytokinin in the root cortex leading to pseudonodule development. Front Plant Sci. 2018;9:1901.
64. Liu H, Sandal N, Andersen KR, James EK, Stougaard J, Kelly S, Kawaharada Y. A genetic screen for plant mutants with altered nodulation phenotypes in response to rhizobial glycan mutants. New Phytol. 2018;220:526–38.
65. Triozzi PM, Irving TB, Schmidt HW, Keyser ZP, Chakraborty S, Balmant K, Pereira WJ, Dervinis C, Mysore KS, Wen J, et al. Spatiotemporal cytokinin response imaging and ISOPENTENYLTRANSFERASE 3 function in Medicago nodule development. Plant Physiol. 2022;188:560–75.
66. Pils B, Heyl A. Unraveling the evolution of cytokinin signaling. Plant Physiol. 2009;151:782–91.
67. Ane JM, Levy J, Thoquet P, Kulikova O, de Billy F, Penmetsa V, Kim DJ, Debelle F, Rosenberg C, Cook DR, et al. Genetic and cytogenetic mapping of DMI1, DMI2, and DMI3 genes of Medicago truncatula involved in Nod factor transduction, nodulation, and mycorrhization. Mol Plant Microbe Interact. 2002;15:1108–18.
68. Stracke S, Kistner C, Yoshida S, Mulder L, Sato S, Kaneko T, Tabata S, Sandal N, Stougaard J, Szczyglowski K, et al. A plant receptor-like kinase required for both bacterial and fungal symbiosis. Nature. 2002;417:959–62.
69. Radutoiu S, Madsen LH, Madsen EB, Felle HH, Umehara Y, Gronlund M, Sato S, Nakamura Y, Tabata S, Sandal N, et al. Plant recognition of symbiotic bacteria requires two LysM receptor-like kinases. Nature. 2003;425:585–92.
70. Sieberer BJ, Chabaud M, Fournier J, Timmers AC, Barker DG. A switch in Ca2+ spiking signature is concomitant with endosymbiotic microbe entry into cortical root cells of Medicago truncatula. Plant J. 2012;69:822–30.
71. Gonzalez-Rizzo S, Crespi M, Frugier F. The Medicago truncatula CRE1 cytokinin receptor regulates lateral root development and early symbiotic interaction with Sinorhizobium meliloti. Plant Cell. 2006;18:2680–93.
72. Miri M, Janakirama P, Huebert T, Ross L, McDowell T, Orosz K, Markmann K, Szczyglowski K. Inside out: root cortex-localized LHK1 cytokinin receptor limits epidermal infection of Lotus japonicus roots by Mesorhizobium loti. New Phytol. 2019;222:1523–37.
73. Fonouni-Farde C, Kisiala A, Brault M, Emery RJN, Diet A, Frugier F. DELLA1-Mediated Gibberellin Signaling Regulates Cytokinin-Dependent Symbiotic Nodulation. Plant Physiol. 2017;175:1795–806.
74. Tirichine L, James EK, Sandal N, Stougaard J. Spontaneous root-nodule formation in the model legume Lotus japonicus: a novel class of mutants nodulates in the absence of rhizobia. Mol Plant Microbe Interact. 2006;19:373–82.
75. Yoro E, Suzaki T, Toyokura K, Miyazawa H, Fukaki H, Kawaguchi M. A positive regulator of nodule organogenesis, nodule inception, acts as a negative regulator of rhizobial infection in Lotus japonicus. Plant Physiol. 2014;165:747–58.
76. Gaudioso-Pedraza R, Beck M, Frances L, Kirk P, Ripodas C, Niebel A, Oldroyd GED, Benitez-Alfonso Y, de Carvalho-Niebel F. Callose-regulated symplastic communication coordinates symbiotic root nodule development. Curr Biol. 2018;28(3562–3577):e3566.
77. Marin-de la Rosa N, Pfeiffer A, Hill K, Locascio A, Bhalerao RP, Miskolczi P, Gronlund AL, Wanchoo-Kohli A, Thomas SG, Bennett MJ, et al. Genome wide binding site analysis reveals transcriptional coactivation of Cytokinin-responsive genes by DELLA proteins. PLoS Genet. 2015;11:e1005337.
78. Hirsch S, Kim J, Munoz A, Heckmann AB, Downie JA, Oldroyd GED. GRAS proteins form a DNA binding complex to induce gene expression during nodulation signaling in Medicago truncatula. Plant Cell. 2009;21:545–57.
79. Jin Y, Liu H, Luo DX, Yu N, Dong WT, Wang C, Zhang XW, Dai HL, Yang J, Wang ET. DELLA proteins are common components of symbiotic rhizobial and mycorrhizal signalling pathways. Nat Commun. 2016;7:12433.
80. Hakoshima T. Structural basis of the specific interactions of GRAS family proteins. FEBS Lett. 2018;592:489–501.
81. Khan Y, Xiong Z, Zhang H, Liu S, Yaseen T, Hui T. Expression and roles of GRAS gene family in plant growth, signal transduction, biotic and abiotic stress resistance and symbiosis formation-a review. Plant Biol (Stuttg). 2022;24:404–16.
82. Broughton WJ, Dilworth MJ. Control of leghaemoglobin synthesis in snake beans. Biochem J. 1971;125:1075–80.
83. Díaz CL, Grønlund M, Schlaman HRM, Spaink HP. Induction of hairy roots for symbiotic gene expression studies. In: Márquez AJ, editors. Lotus japonicus Handbook. Dordrecht: Springer. 2005. p. 261–277. https://doi.org/10.1007/1-4020-3735-X_26.
84. Berardini TZ, Reiser L, Li D, Mezheritsky Y, Muller R, Strait E, Huala E. The Arabidopsis information resource: making and mining the "gold standard" annotated reference plant genome. Genesis. 2015;53:474–85.
85. Sato S, Nakamura Y, Kaneko T, Asamizu E, Kato T, Nakao M, Sasamoto S, Watanabe A, Ono A, Kawashima K, et al. Genome structure of the legume, Lotus japonicus. DNA Res. 2008;15:227–39.
86. Goodstein DM, Shu S, Howson R, Neupane R, Hayes RD, Fazo J, Mitros T, Dirks W, Hellsten U, Putnam N, et al. Phytozome: a comparative platform for green plant genomics. Nucleic Acids Res. 2012;40:D1178-1186.
87. Tang H, Krishnakumar V, Bidwell S, Rosen B, Chan A, Zhou S, Gentzbittel L, Childs KL, Yandell M, Gundlach H, et al. An improved genome release (version Mt4.0) for the model legume Medicago truncatula. BMC Genomics. 2014;15:312.
88. Frazer KA, Pachter L, Poliakov A, Rubin EM, Dubchak I. VISTA: computational tools for comparative genomics. Nucleic Acids Res. 2004;32:W273-279.
89. Brudno M, Malde S, Poliakov A, Do CB, Couronne O, Dubchak I, Batzoglou S. Glocal alignment: finding rearrangements during alignment. Bioinformatics. 2003;19(Suppl 1):i54-62.
90. Maekawa T, Kusakabe M, Shimoda Y, Sato S, Tabata S, Murooka Y, Hayashi M. Polyubiquitin promoter-based binary vectors for overexpression and gene silencing in Lotus japonicus. Mol Plant Microbe Interact. 2008;21:375–82.
91. Yu H, Xiao A, Wu J, Li H, Duan Y, Chen Q, Zhu H, Cao Y. GmNAC039 and GmNAC018 activate the expression of cysteine protease genes to promote soybean nodule senescence. Plant Cell. 2023;35:2929–51.
92. Hellens RP, Allan AC, Friel EN, Bolitho K, Grafton K, Templeton MD, Karunairetnam S, Gleave AP, Laing WA. Transient expression vectors for functional genomics, quantification of promoter activity and RNA silencing in plants. Plant Methods. 2005;1:13.
93. Wang Y, Luo M. Random DNA Binding Selection Assay (RDSA). Bio-Protoc. 2015;5:e1452.

Publisher's Note